

# Klimaänderung I

## 1. Rahmen, Kontext, Methoden

Robert Sausen

Institut für Physik der Atmosphäre  
Deutsches Zentrum für Luft- und Raumfahrt  
Oberpfaffenhofen

Vorlesung WS 2022/23

LMU München



## Technical information

- <http://www.pa.op.dlr.de/~RobertSausen/vorlesung/index.html>
  - Most recent update on the lecture
  - Slides of the lecture (with some delay)
  
  - See also LSF <https://lsf.verwaltung.uni-muenchen.de/>
  
- Contact: robert.sausen@dlr.de
  
- Further information:
  - [www.ipcc.ch](http://www.ipcc.ch)
  - [www.de-ipcc.de](http://www.de-ipcc.de)

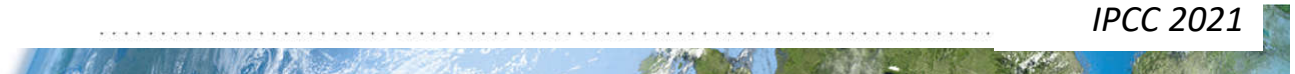


# Contents of IPCC AR 6 2021: Working Group I: the Physical Science Basis

## Chapters

<b>Chapter 1</b>	Framing, Context, and Methods .....
<b>Chapter 2</b>	Changing State of the Climate System .....
<b>Chapter 3</b>	Human Influence on the Climate System .....
<b>Chapter 4</b>	Future Global Climate: Scenario-based Projections and Near-term Information ...
<b>Chapter 5</b>	Global Carbon and Other Biogeochemical Cycles and Feedbacks .....
<b>Chapter 6</b>	Short-lived Climate Forcers .....
<b>Chapter 7</b>	The Earth's Energy Budget, Climate Feedbacks and Climate Sensitivity .....
<b>Chapter 8</b>	Water Cycle Changes .....
<b>Chapter 9</b>	Ocean, Cryosphere and Sea Level Change .....
<b>Chapter 10</b>	Linking Global to Regional Climate Change .....
<b>Chapter 11</b>	Weather and Climate Extreme Events in a Changing Climate .....
<b>Chapter 12</b>	Climate Change Information for Regional Impact and for Risk Assessment .....
<b>Atlas</b>	.....

IPCC 2021



## General structure of chapter

- Coordinating Lead Authors
- Lead Authors
- Contributing Authors
- Review Editors
- Chapter Scientists
- Table of Contents
- Executive Summary
- **Sections**
  - Boxes
- Acknowledgements
- Frequently Asked Questions
- References
- Appendices



# Chapter 1: Framing, context, and methods

## Coordinating Lead Authors:

Deliang Chen (Sweden), Maisa Rojas (Chile), Bjørn H. Samset (Norway)

## Lead Authors:

Kim Cobb (United States of America), Aida Diongue-Niang (Senegal), Paul Edwards (United States of America), Seita Emori (Japan), Sergio Henrique Faria (Spain/Brazil), Ed Hawkins (United Kingdom), Pandora Hope (Australia), Philippe Huybrechts (Belgium), **Malte Meinshausen (Australia/Germany)**, Sawsan Khair Elsied Abdel Rahim Mustafa (Sudan), Gian-Kasper Plattner (Switzerland), Anne Marie Treguier (France)

# Chapter 1: Framing, context, and methods

## Contributing Authors:

Hui-Wen Lai (Sweden), Tania Villaseñor (Chile), Rondrotiana Barimalala (South Africa/Madagascar), Rosario Carmona (Chile), Peter M. Cox (United Kingdom), **Wolfgang Cramer (France/Germany)**, Francisco J. Doblas-Reyes (Spain), Hans Dolman (The Netherlands), Alessandro Dosio (Italy), **Veronika Eyring (Germany)**, Gregory M. Flato (Canada), Piers Forster (United Kingdom), David Frame (New Zealand), **Katja Frieler (Germany)**, Jan S. Fuglestad (Norway), John C. Fyfe (Canada), **Mathias Garschagen (Germany)**, Joelle Gergis (Australia), Nathan P. Gillett (Canada), Michael Grose (Australia), Eric Guilyardi (France), Celine Guivarch (France), Susan Hassol (United States of America), Zeke Hausfather (United States of America), Hans Hersbach (United Kingdom/The Netherlands), Helene T. Hewitt (United Kingdom), Mark Howden (Australia), Christian Huggel (Switzerland), Margot Hurlbert (Canada), Christopher Jones (United Kingdom), Richard G. Jones (United Kingdom), Darrell S. Kaufman (United States of America), Robert E. Kopp (United States of America), Anthony Leiserowitz (United States of America), Robert J. Lempert (United States of America), Jared Lewis (Australia/New Zealand), Hong Liao (China), Nikki Lovenduski (United States of America), Marianne T. Lund (Norway), Katharine Mach (United States of America), Douglas Maraun (Austria/Germany), **Jochem Marotzke (Germany)**, **Jan Minx (Germany)**, Zebedee R.J. Nicholls (Australia), Brian C. O'Neill (United States of America), M. Giselle Ogaz (Chile), **Friederike Otto (United Kingdom /Germany)**, Wendy Parker (United Kingdom), Camille Parmesan (France, United Kingdom/United States of America), Warren Pearce (United Kingdom), Roque Pedace (Argentina), Andy Reisinger (New Zealand), James Renwick (New Zealand), Keywan Riahi (Austria), Paul Ritchie (United Kingdom), Joeri Rogelj (United Kingdom/Belgium), Rodolfo Sapiains (Chile), Yusuke Satoh (Japan), Sonia I. Seneviratne (Switzerland), Theodore G. Shepherd (United Kingdom/Canada), **Jana Sillmann (Norway/Germany)**, Lucas Silva (Portugal/Switzerland), Aimée B.A. Slangen (The Netherlands), Anna A. Sörensson (Argentina), Peter Steinle (Australia), Thomas F. Stocker (Switzerland), **Martina Stockhause (Germany)**, Daithi Stone (New Zealand), Abigail Swann (United States of America), Sophie Szopa (France), Izuru Takayabu (Japan), Claudia Tebaldi (United States of America), Laurent Terray (France), Peter W. Thorne (Ireland/ United Kingdom), Blair Trewin (Australia), Isabel Trigo Portugal), Maarten K. van Aalst (The Netherlands), Bart van den Hurk (The Netherlands), Detlef van Vuuren (The Netherlands), Robert Vautard (France), Carolina Vera (Argentina), David Viner (United Kingdom), **Axel von Engeln (Germany)**, **Karina von Schuckmann (France/Germany)**, Xuebin Zhang (Canada)

IPCC AR6 WG I, 2021, Chapter 1



# Chapter 1: Framing, context, and methods

## Review Editors:

Nares Chuersuwat (Thailand), **Gabriele Hegerl (United Kingdom/Germany)**, Tetsuzo Yasunari (Japan)



## Statements in the Executive Summary

Working Group I (WGI) of the Intergovernmental Panel on Climate Change (IPCC) assesses the current evidence on the physical science of climate change, evaluating knowledge gained from observations, reanalyses, paleoclimate archives and climate model simulations, as well as physical, chemical and biological climate processes. This chapter sets the scene for the WGI assessment, placing it in the context of ongoing global and regional changes, international policy responses, the history of climate science and the evolution from previous IPCC assessments, including the Special Reports prepared as part of this Assessment Cycle. Key concepts and methods, relevant recent developments, and the modelling and scenario framework used in this assessment are presented.





# Statements in the Executive Summary

## Framing and Context of the WGI Report (1)

**The WGI contribution to the IPCC Sixth Assessment Report (AR6) assesses new scientific evidence relevant for a world whose climate system is rapidly changing, overwhelmingly due to human influence.** The five IPCC assessment cycles since 1990 have comprehensively and consistently laid out the rapidly accumulating evidence of a changing climate system, with the Fourth Assessment Report (AR4, 2007) being the first to conclude that warming of the climate system is unequivocal. Sustained changes have been documented in all major elements of the climate system, including the atmosphere, land, cryosphere, biosphere and ocean. Multiple lines of evidence indicate the unprecedented nature of recent large-scale climatic changes in context of all human history, and that they represent a millennial-scale commitment for the slow-responding elements of the climate system, resulting in continued worldwide loss of ice, increase in ocean heat content, sea level rise and deep ocean acidification. {1.2.1, 1.3, Box 1.2, Appendix 1.A}





# The structure of the AR6 WGI Report

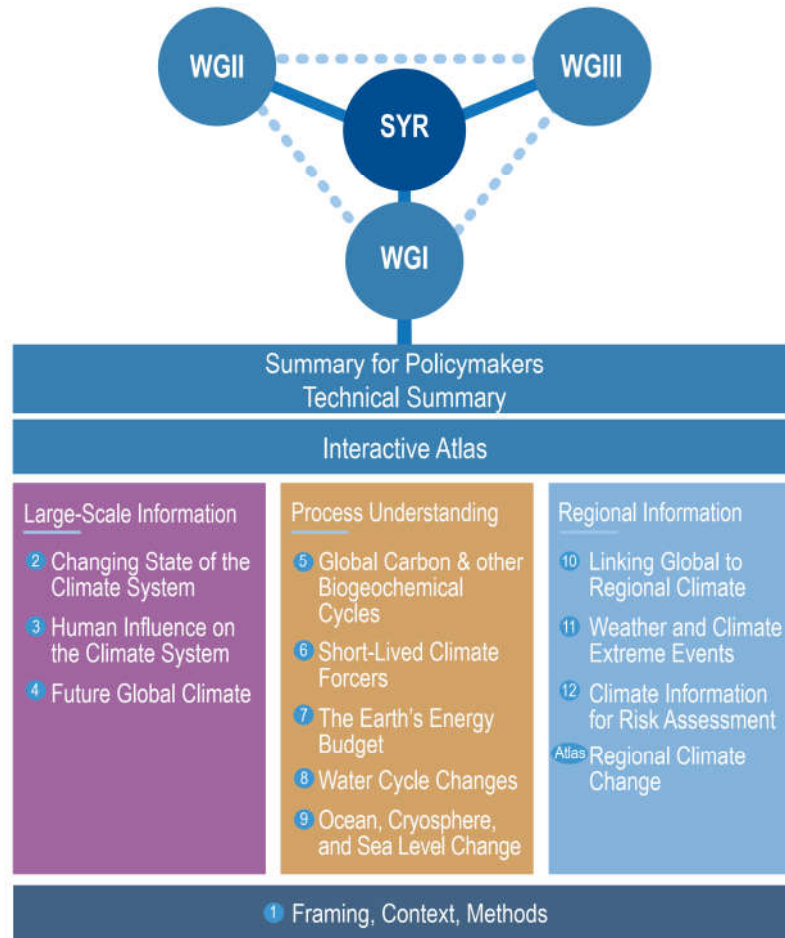


**Figure 1.1 | The structure of the AR6 WGI Report.** Shown are the three pillars of the AR6 WGI, its relation to the WGII and WGIII contributions, and the cross-working-group AR6 Synthesis Report (SYR).





## The structure of the AR6 WGI Report

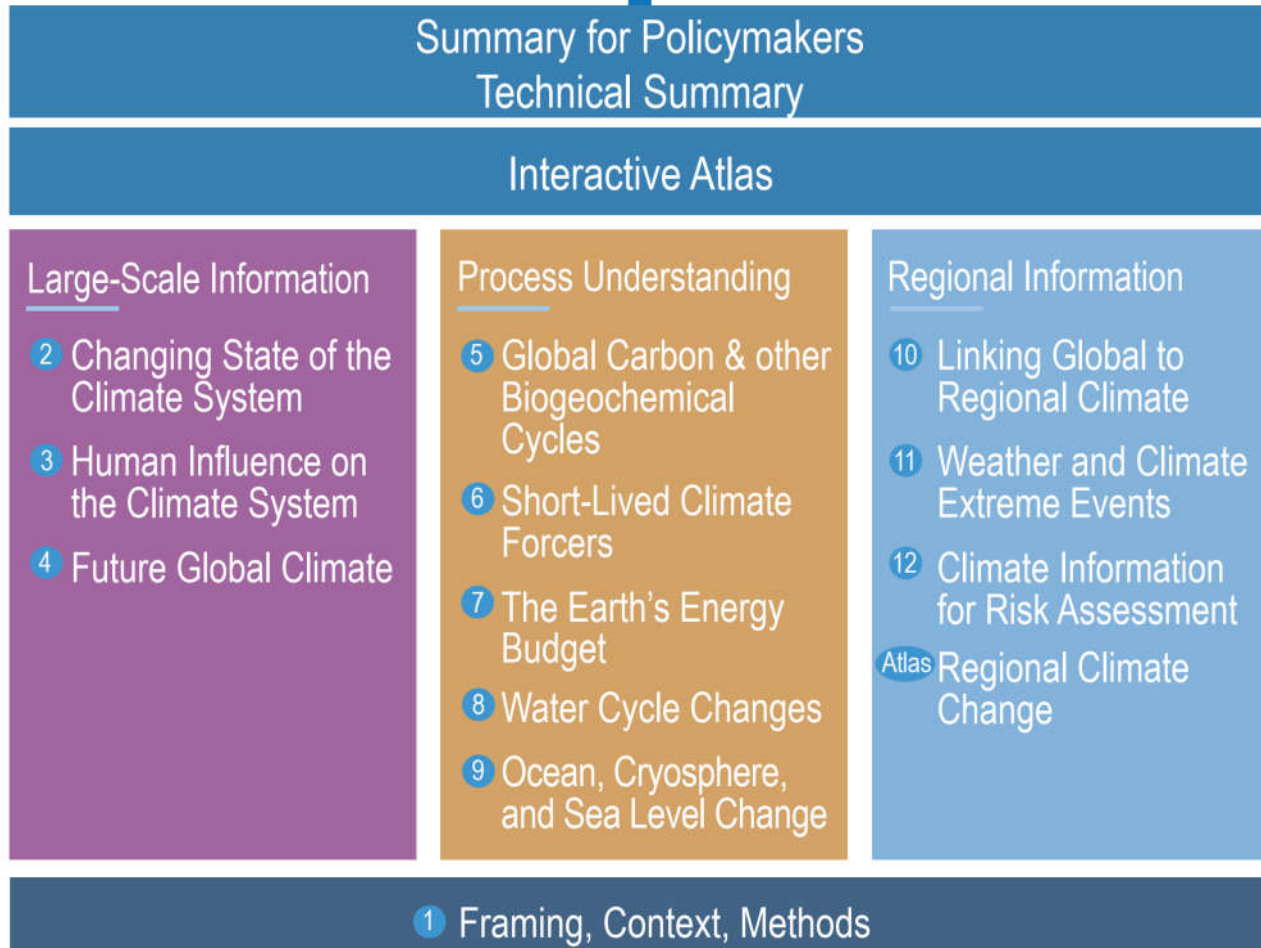


**Figure 1.1 | The structure of the AR6 WGI Report.** Shown are the three pillars of the AR6 WGI, its relation to the WGII and WGIII contributions, and the cross-working-group AR6 Synthesis Report (SYR).

# Main relations between AR5 WGI and AR6 WGI chapters

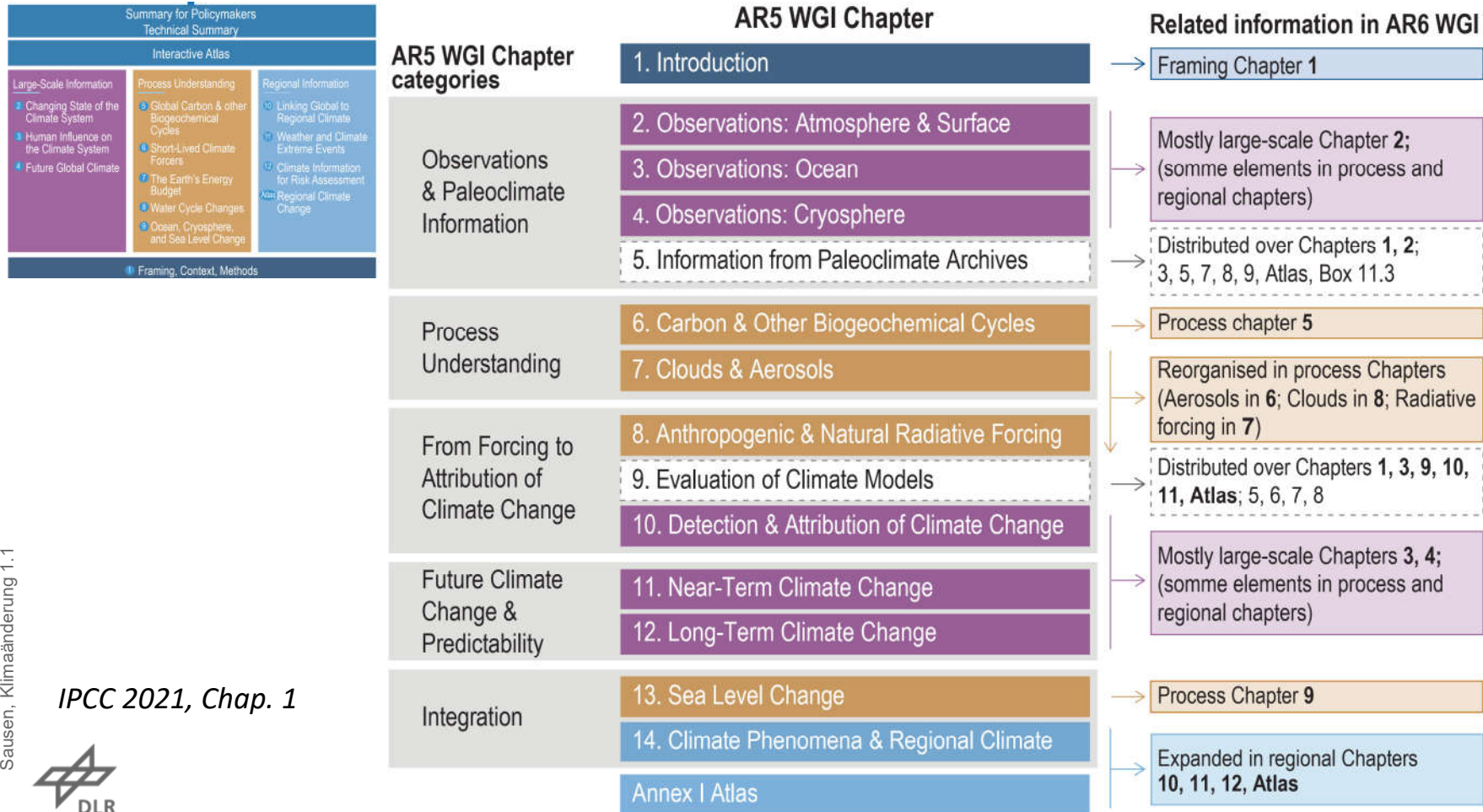


**Figure 1.2 | Main relations between AR5 WGI and AR6 WGI chapters.** The left-hand column shows the AR5 WGI chapter categories. The central column lists the AR5 WGI chapters, with the colour code indicating their relation to the AR6 WGI structure shown in Figure 1.1: Large-Scale Information (purple), Process Understanding (gold), Regional Information (light blue) and Whole-Report Information (dark blue). AR5 WGI chapters depicted in white have their topics distributed over multiple AR6 WGI chapters and categories. The right-hand column explains where to find related information in the AR6 WGI report.

# Statements in the Executive Summary

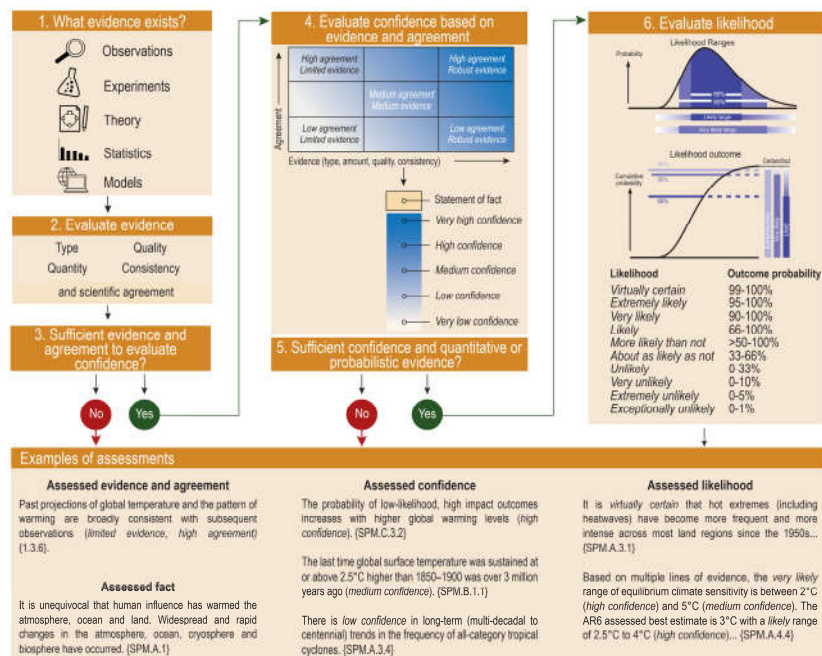
## Framing and Context of the WGI Report (2)

**Since the IPCC Fifth Assessment Report (AR5), the international policy context of IPCC reports has changed.** The UN Framework Convention on Climate Change (UNFCCC, 1992) has the overarching objective of preventing ‘dangerous anthropogenic interference with the climate system’. Responding to that objective, the Paris Agreement (2015) established the long-term goals of ‘holding the increase in global average temperature to well below 2°C above pre-industrial levels and pursuing efforts to limit the temperature increase to 1.5°C above pre-industrial levels’ and of achieving ‘a balance between anthropogenic emissions by sources and removals by sinks of greenhouse gases in the second half of this century’. Parties to the Agreement have submitted Nationally Determined Contributions (NDCs) indicating their planned mitigation and adaptation strategies. However, the NDCs submitted as of 2020 are insufficient to reduce greenhouse gas emission enough to be consistent with trajectories limiting global warming to well below 2°C above pre-industrial levels (*high confidence*). {1.1, 1.2}



# Characterizing understanding and uncertainty in assessment findings

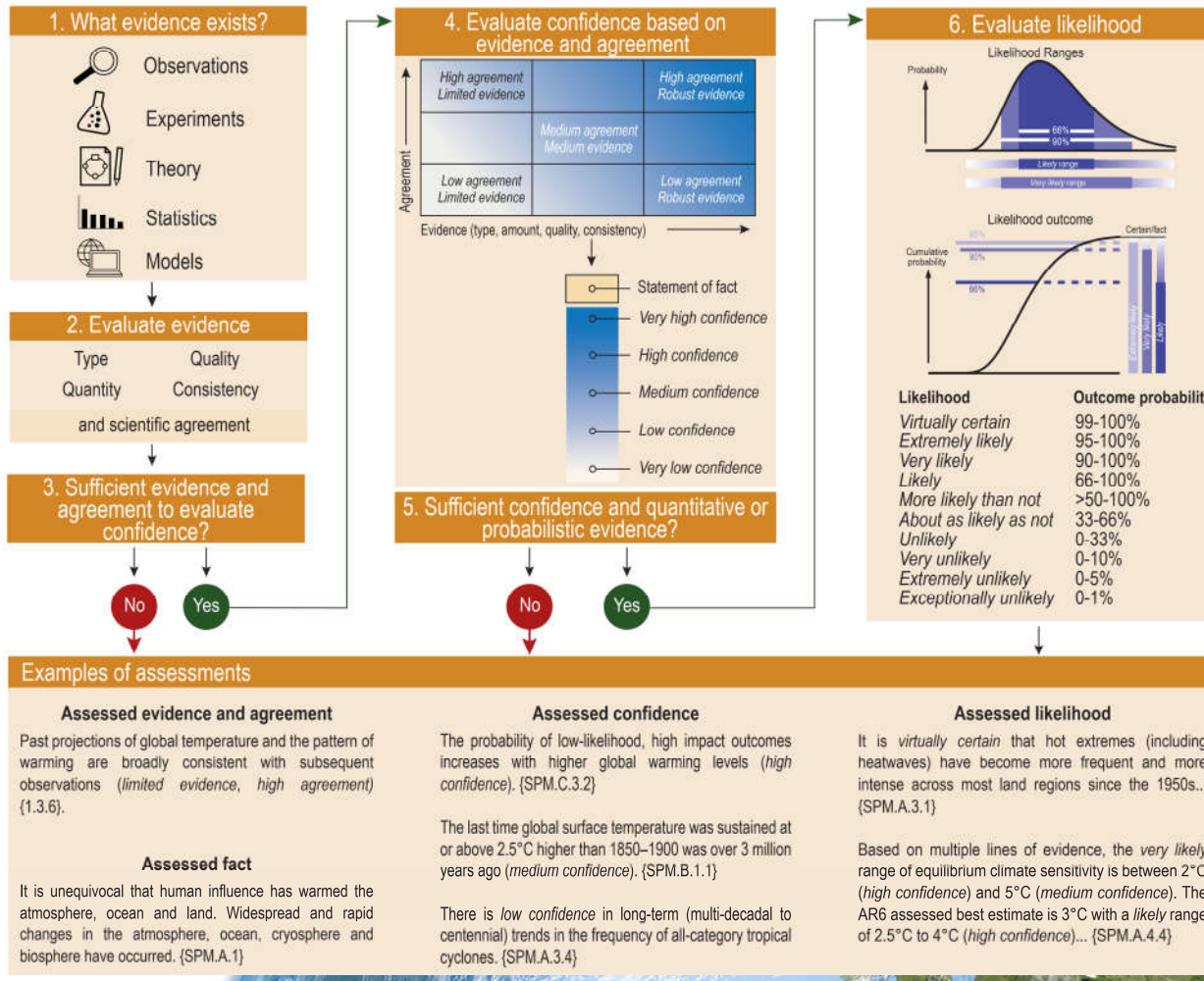
Evaluation and communication of degree of certainty in AR6 findings

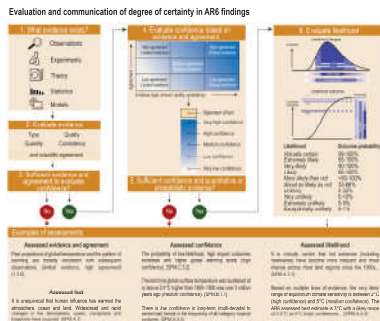


**Box 1.1, Figure 1 | The IPCC AR6 approach for characterizing understanding and uncertainty in assessment findings.** This diagram illustrates the step-by-step process authors use to evaluate and communicate the state of knowledge in their assessment (Mastrandrea et al., 2010). Authors present evidence/agreement, confidence, or likelihood terms with assessment conclusions, communicating their expert judgments accordingly. Example conclusions drawn from Report are presented in the box at the bottom of the figure. Figure adapted from Mach et al. (2017) .



## Evaluation and communication of degree of certainty in AR6 findings





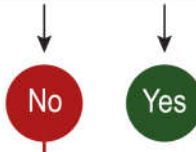
## 1. What evidence exists?

- Observations
- Experiments
- Theory
- Statistics
- Models

## 2. Evaluate evidence

- Type
- Quality
- Quantity
- Consistency
- and scientific agreement

## 3. Sufficient evidence and agreement to evaluate confidence?



## Examples of assessments

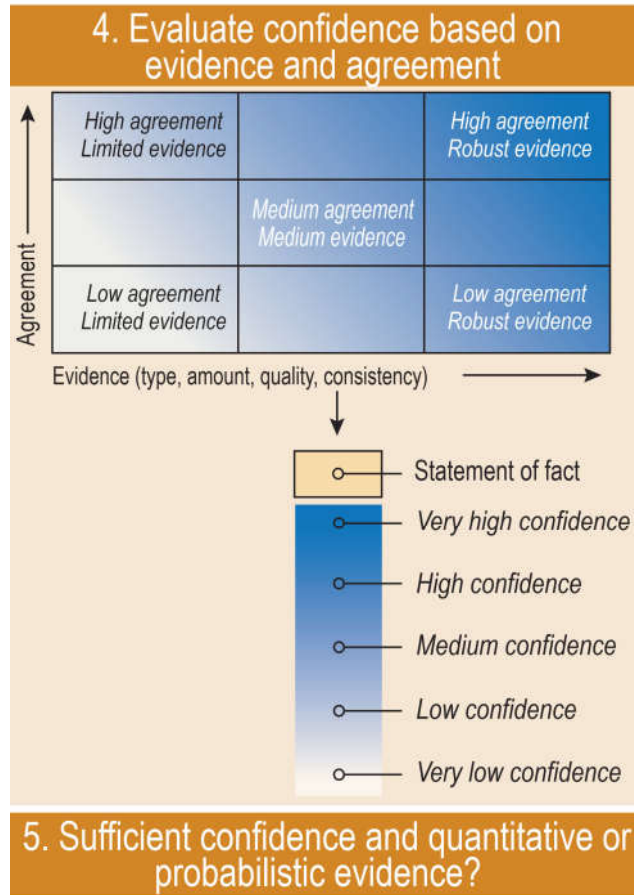
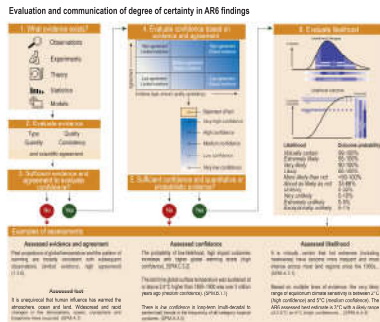
### Assessed evidence and agreement

Past projections of global temperature and the pattern of warming are broadly consistent with subsequent observations (*limited evidence, high agreement*) {1.3.6}.

### Assessed fact

It is unequivocal that human influence has warmed the atmosphere, ocean and land. Widespread and rapid changes in the atmosphere, ocean, cryosphere and biosphere have occurred. {SPM.A.1}





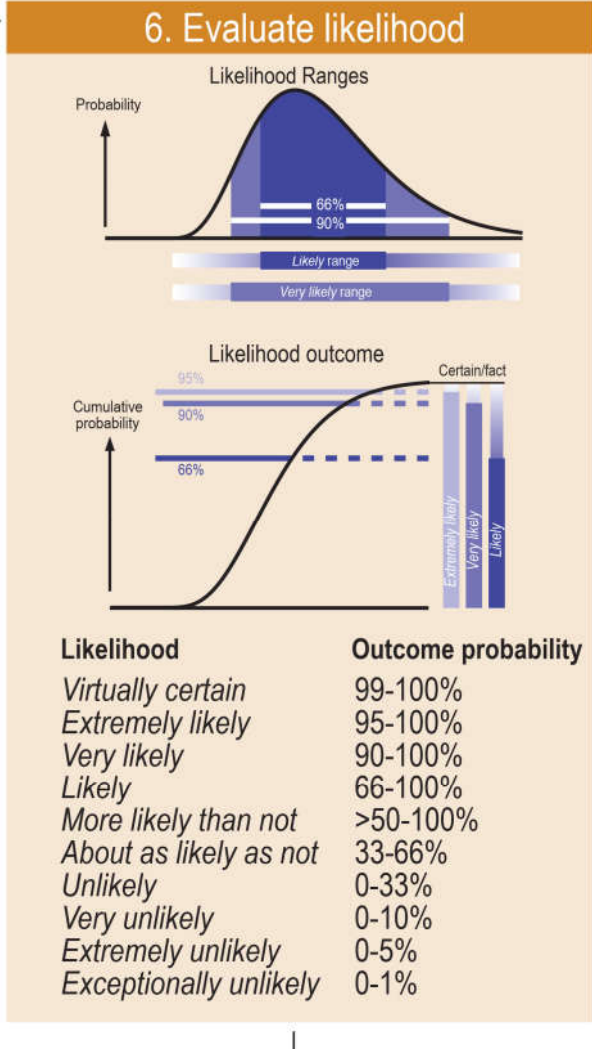
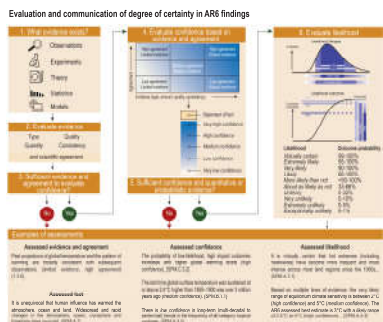
## Assessed confidence

The probability of low-likelihood, high impact outcomes increases with higher global warming levels (*high confidence*). {SPM.C.3.2}

The last time global surface temperature was sustained at or above 2.5°C higher than 1850–1900 was over 3 million years ago (*medium confidence*). {SPM.B.1.1}

There is *low confidence* in long-term (multi-decadal to centennial) trends in the frequency of all-category tropical cyclones. {SPM.A.3.4}





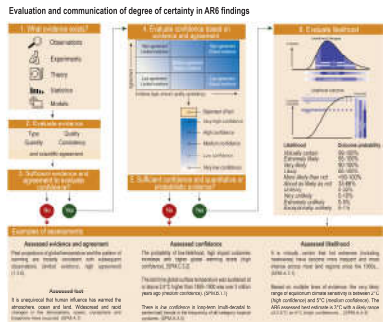
↓

## Assessed likelihood

It is *virtually certain* that hot extremes (including heatwaves) have become more frequent and more intense across most land regions since the 1950s... {SPM.A.3.1}

Based on multiple lines of evidence, the *very likely* range of equilibrium climate sensitivity is between 2°C (*high confidence*) and 5°C (*medium confidence*). The AR6 assessed best estimate is 3°C with a *likely* range of 2.5°C to 4°C (*high confidence*)... {SPM.A.4.4}





### 4. Evaluate confidence based on evidence and agreement

Agreement ↑	High agreement Limited evidence	High agreement Robust evidence
	Medium agreement Medium evidence	
	Low agreement Limited evidence	Low agreement Robust evidence

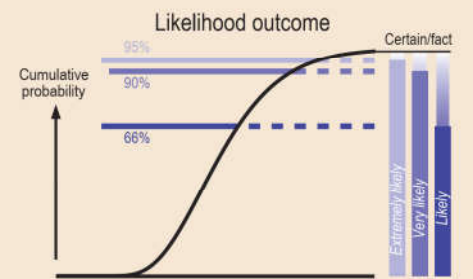
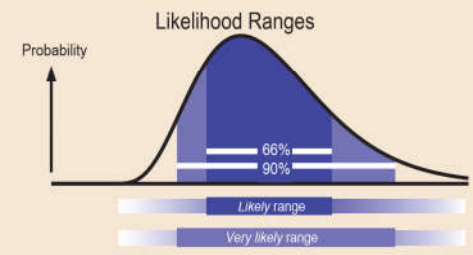
Evidence (type, amount, quality, consistency) →

- Statement of fact
- Very high confidence
- High confidence
- Medium confidence
- Low confidence
- Very low confidence

### 5. Sufficient confidence and quantitative or probabilistic evidence?



### 6. Evaluate likelihood



Likelihood	Outcome probability
Virtually certain	99-100%
Extremely likely	95-100%
Very likely	90-100%
Likely	66-100%
More likely than not	>50-100%
About as likely as not	33-66%
Unlikely	0-33%
Very unlikely	0-10%
Extremely unlikely	0-5%
Exceptionally unlikely	0-1%

# Statements in the Executive Summary

## Framing and Context of the WGI Report (3)

**This report provides information of potential relevance to the 2023 global stocktake.**

The 5-yearly stocktakes called for in the Paris Agreement will evaluate alignment among the Agreement's long-term goals, its means of implementation and support, and evolving global efforts in climate change mitigation (efforts to limit climate change) and adaptation (efforts to adapt to changes that cannot be avoided). In this context, WGI assesses, among other topics, remaining cumulative carbon emission budgets for a range of global warming levels, effects of long-lived and short-lived climate forcers, projected changes in sea level and extreme events, and attribution to anthropogenic climate change. {Cross-Chapter Box 1.1}



# Statements in the Executive Summary

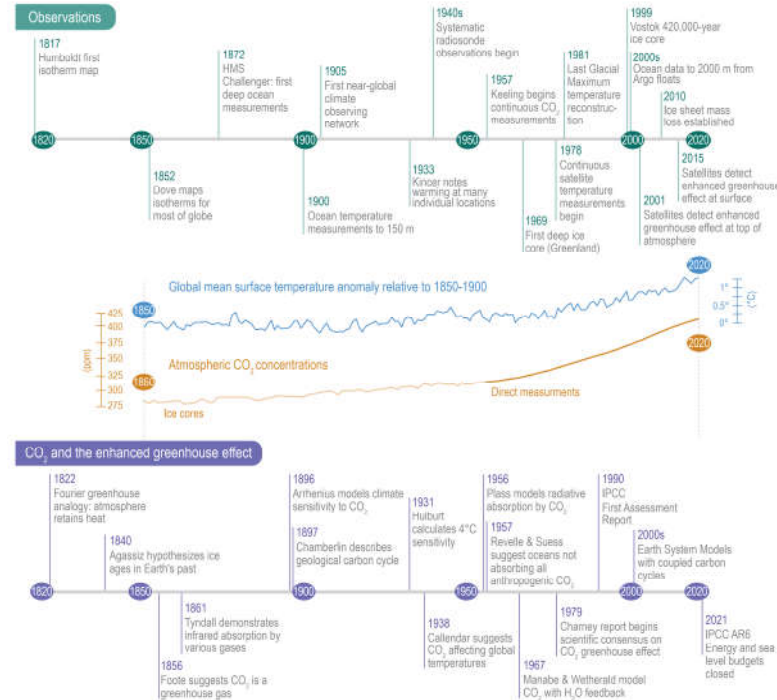
## Framing and Context of the WGI Report (4)

**Understanding of the fundamental features of the climate system is robust and well established.** Scientists in the 19th-century identified the major natural factors influencing the climate system. They also hypothesized the potential for anthropogenic climate change due to carbon dioxide (CO<sub>2</sub>) emitted by fossil fuel combustion. The principal natural drivers of climate change, including changes in incoming solar volcanic activity, orbital cycles, and changes in global biogeochemical cycles, have been studied systematically since the early 20th century. Other major anthropogenic drivers, such as atmospheric aerosols (fine solid particles or liquid droplets), land-use change and non-CO<sub>2</sub> greenhouse gases, were identified by the 1970s. Since systematic scientific assessments began in the 1970s, the influence of human activity on the warming of the climate system has evolved from theory to established fact. Past projections of global surface temperature and the pattern of warming are broadly consistent with subsequent observations (*limited evidence, high agreement*), especially when accounting for the difference in radiative forcing scenarios used for making projections and the radiative forcings that actually occurred. {1.3.1 - 1.3.6}

IPCC 2021, Chap. 1

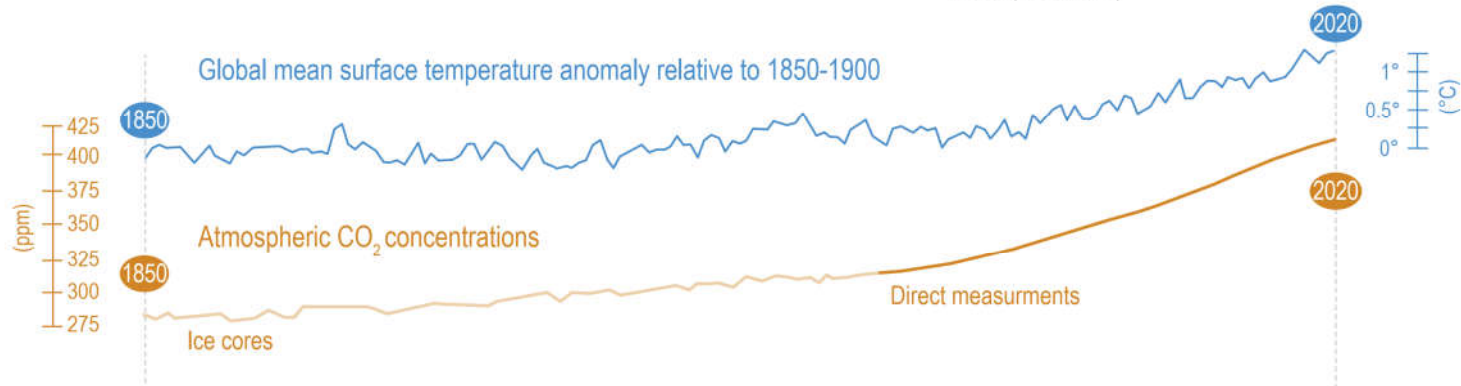
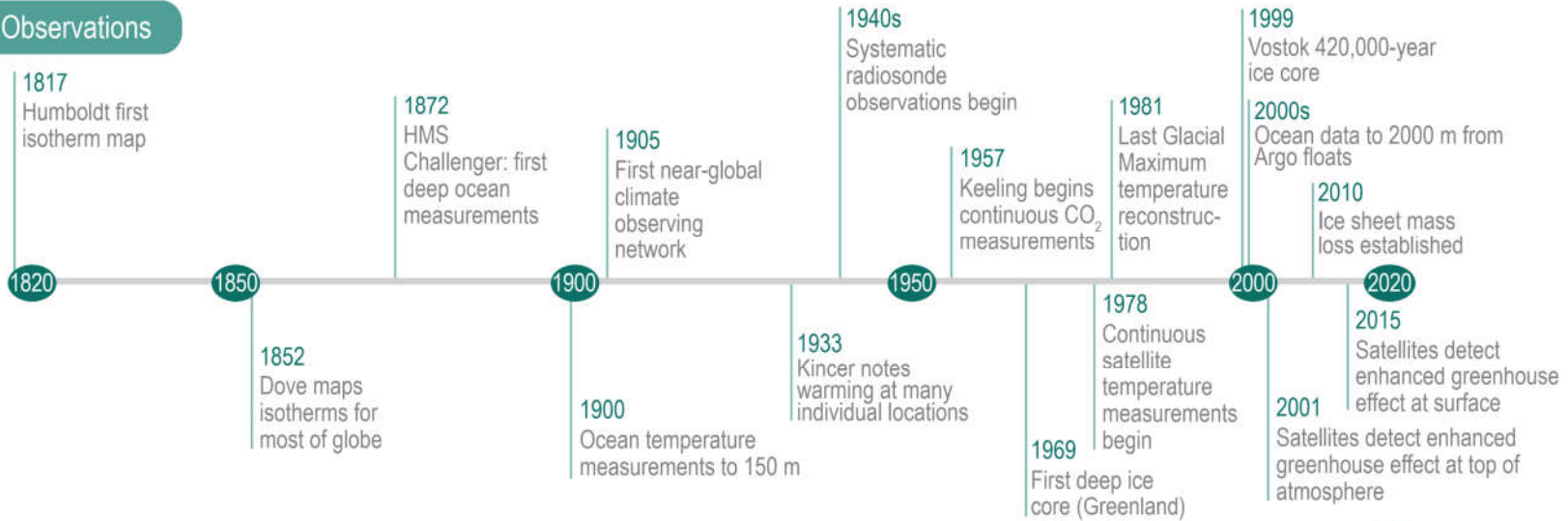


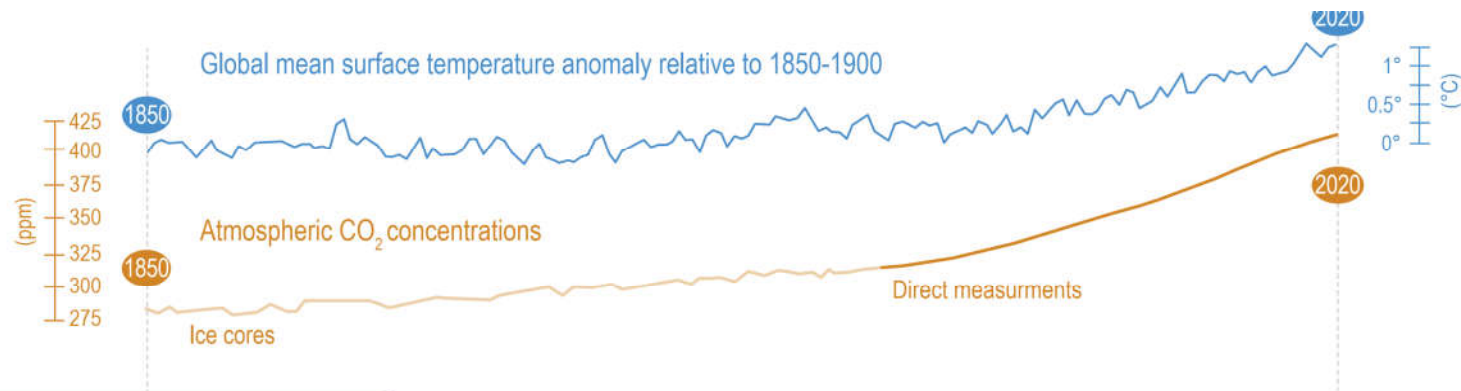
# Climate science milestones between 1817-2021



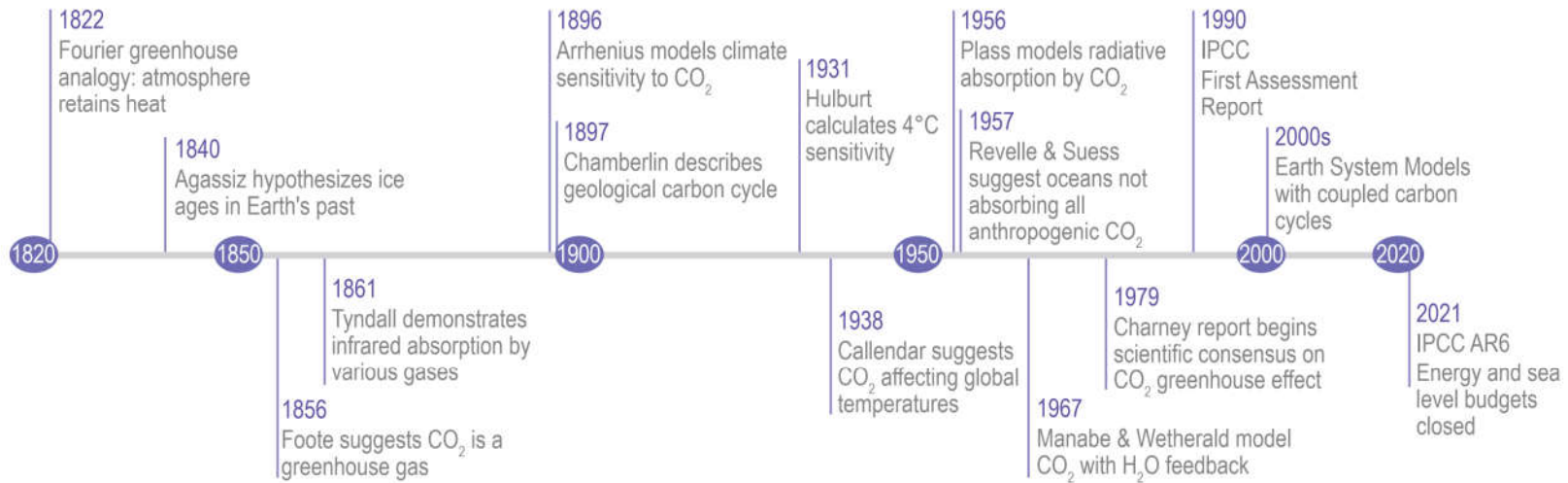
**Figure 1.6 | Climate science milestones, between 1817 and 2021. Top:** Milestones in observations. **Middle:** Curves of global surface air temperature (GMST) anomaly relative to 1850–1900, using HadCRUT5 (Morice et al., 2021); atmospheric CO<sub>2</sub> concentrations from Antarctic ice cores (Lüthi et al., 2008; Bereiter et al., 2015); direct air measurements from 1957 onwards (see Figure 1.4 for details; Tans and Keeling, 2020). **Bottom:** Milestones in scientific understanding of the CO<sub>2</sub>-enhanced greenhouse effect. Further details on each milestone are available in Section 1.3, and in Chapter 1 of AR4 (Le Treut et al., 2007).

## Observations





**CO<sub>2</sub> and the enhanced greenhouse effect**





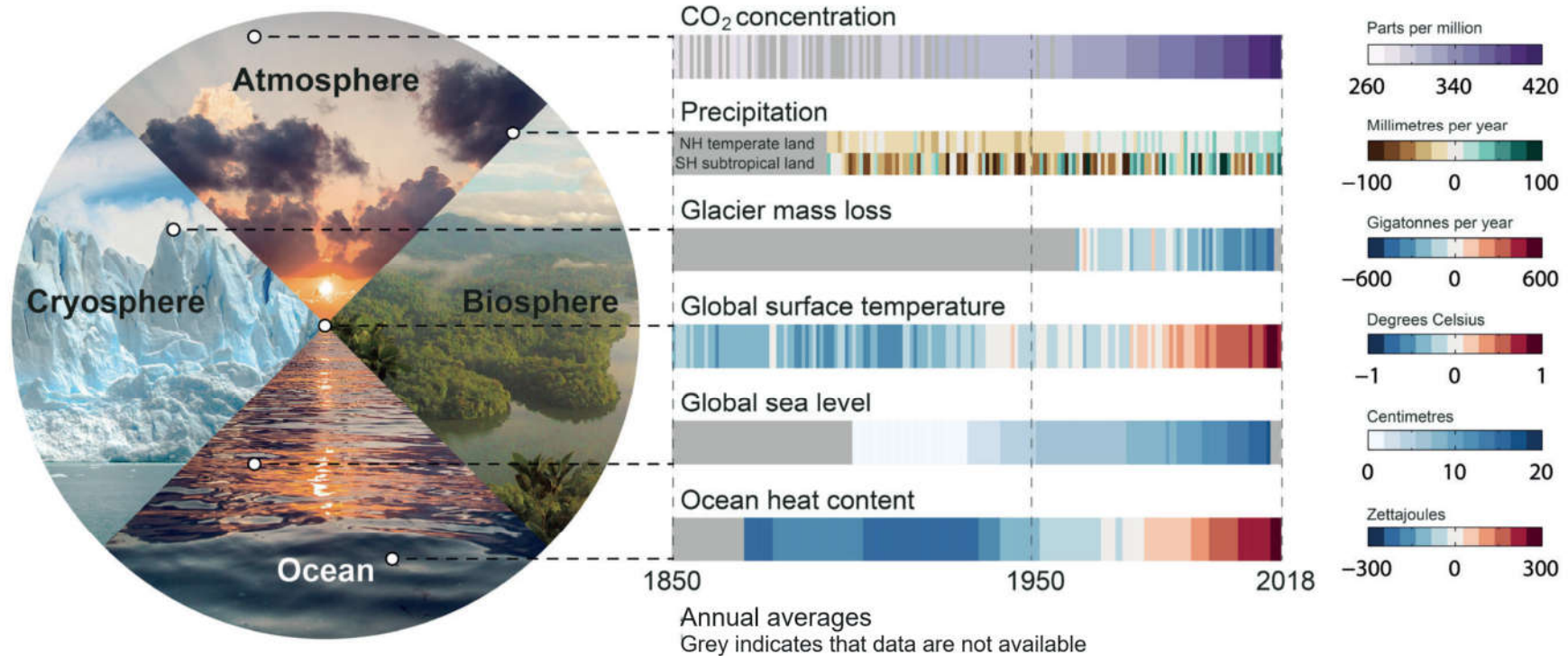
## Statements in the Executive Summary

### Framing and Context of the WGI Report (5)

**Global surface temperatures increased by about 0.1°C (*likely* range –0.1°C to +0.3°C, *medium confidence*) between the period around 1750 and the 1850–1900 period, with anthropogenic factors responsible for a warming of 0.0°C – 0.2°C (*likely range, medium confidence*). This assessed change in temperature before 1850–1900 is not included in the AR6 assessment of global warming to date, to ensure consistency with previous IPCC assessment reports, and because of the lower confidence in the estimate. There was *likely* a net anthropogenic forcing of 0.0 – 0.3 Wm<sup>-2</sup> in 1850–1900 relative to 1750 (*medium confidence*), with radiative forcing from increases in atmospheric greenhouse gas concentrations being partially offset by anthropogenic aerosol emissions and land-use change. Net radiative forcing from solar and volcanic activity is estimated to be smaller than  $\pm 0.1$  Wm<sup>-2</sup> for the same period. {Cross Chapter Box 1.2, 1.4.1, Cross Chapter Box 2.3}**



# Changes are occurring throughout the climate system



IPCC 2021, Chap. 1

**Figure 1.4 | Changes are occurring throughout the climate system.** **Left:** Main realms of the climate system: atmosphere, biosphere, cryosphere and ocean. **Right:** Six key indicators of ongoing changes since 1850, or the start of the observational or assessed record, through 2018. Each stripe indicates the global (except for precipitation which shows two latitude band means), annual mean anomaly for a single year, relative to a multi-year baseline (except for CO<sub>2</sub> concentration and glacier mass loss, which are absolute values). Grey indicates that data are not available. Datasets and baselines used are: (i) CO<sub>2</sub>: Antarctic ice cores (Lüthi et al., 2008; Bereiter et al., 2015) and direct air measurements (Tans and Keeling, 2020) (see Figure 1.5 for details); (ii) precipitation: Global Precipitation Climatology Centre (GPCC) V8 (updated from Becker et al., 2013), baseline 1961–1990 using land areas only with latitude bands 33°N–66°N and 15°S–30°S; (iii) glacier mass loss: Zemp et al. (2019); (iv) global surface air temperature (GMST): HadCRUT5 (Morice et al., 2021), baseline 1961–1990; (v) sea level change: (Dangendorf et al., 2019), baseline 1900–1929; (vi) ocean heat content (model–observation hybrid): Zanna et al. (2019), baseline 1961–1990. Further details on data sources and processing are available in the chapter data table (Table 1.SM.1).

# Jahresmittel der Temperatur am Hohenpeißenberg (seit 1781)

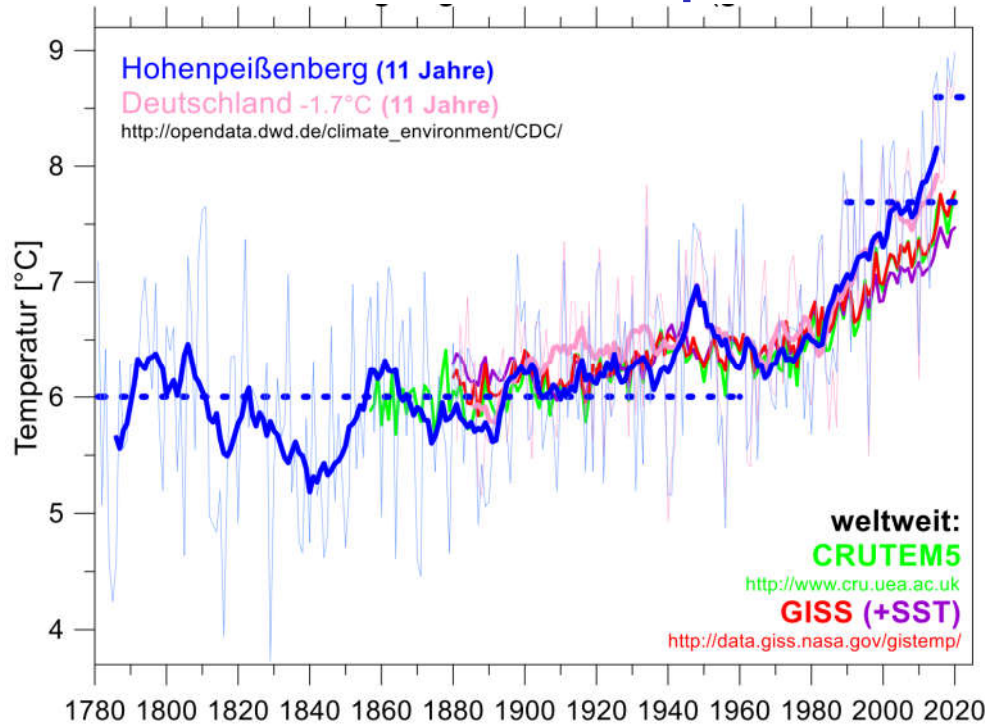


Abbildung 1: Jahresmittel der Temperatur am Hohenpeißenberg (blaue Kurven), sowie über Deutschland (rosa Kurven, um 1.7°C nach unten verschoben). Dünne Linien: Jahresmittel. Dicke Linien: gleitendes Mittel über 11 Jahre. Dicke gestrichelte Linien: langjährige Hohenpeißenberger Mittel der Jahre 1781 bis 1960 (6°C), 1990 bis 2020 (7.7°C) und 2015 bis 2020 (8.6°C). Zum Vergleich sind auch weltweite Temperaturanomalien der Landoberfläche gezeigt (CRUTEM5 und GISS, 6.45°C nach oben verschoben). GISS liefert zusätzlich die weltweite Land- und Meeresoberflächen Temperaturanomalie (+SST). Weitere Informationen siehe angegebene Webseiten, sowie DWD Mitteilung vom Januar 2020.

ca. 1900



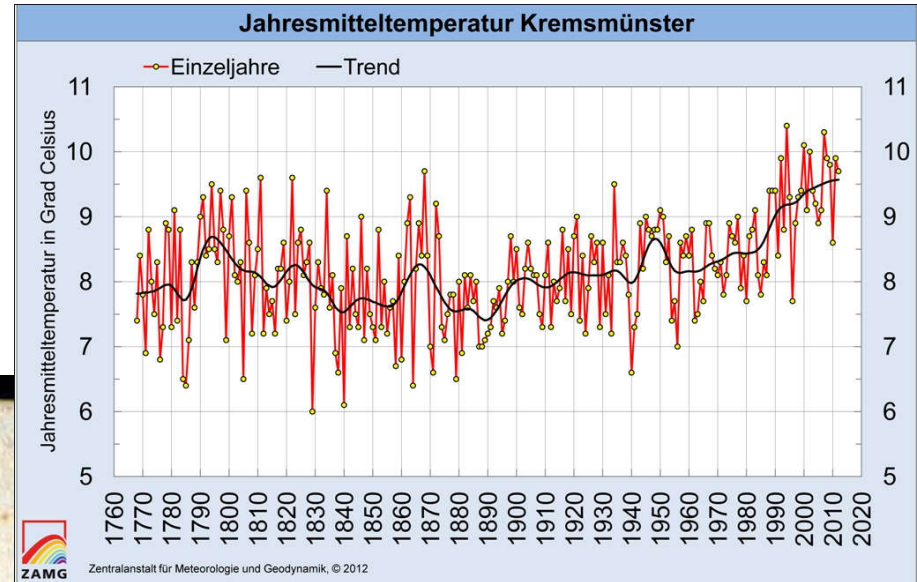
~ heute



# Wetterbeobachtung im Stift Kremsmünster (Österreich), seit 1762



"28. December 1762, frigus maximus, Barometer 27° 2' "



[www.zamg.ac.at](http://www.zamg.ac.at)



# Long-term context of anthropogenic climate change

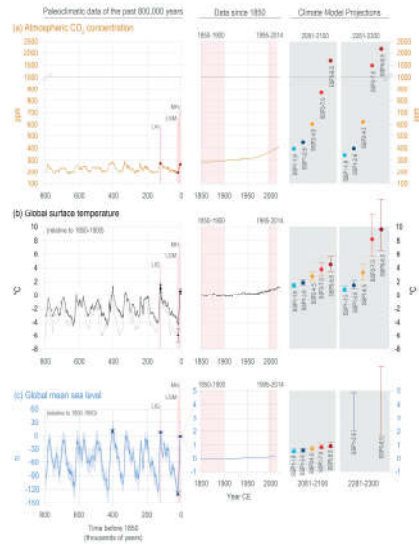


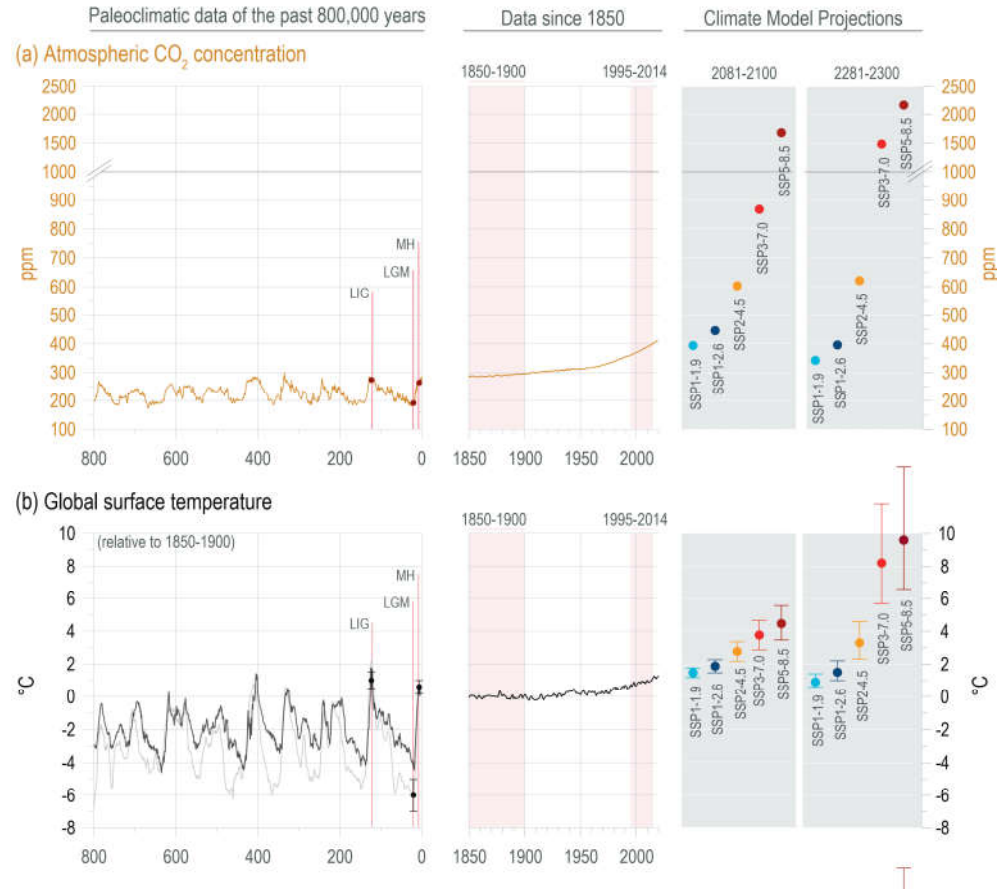
**Figure 1.5 | Long-term context of anthropogenic climate change based on selected paleoclimatic reconstructions over the past 800,000 years (800 kyr) for three key indicators: atmospheric CO<sub>2</sub> concentrations, global mean surface temperature (GMST), and global mean sea level (GMSL).**

**Figure 1.5 (continued): (a) Measurements of CO<sub>2</sub> in air enclosed in Antarctic ice cores** (Lüthi et al., 2008; Bereiter et al., 2015 [a compilation]; uncertainty  $\pm 1.3$  ppm; see Sections 2.2.3 and 5.1.2 for an assessment) **and direct air measurements** (Tans and Keeling, 2020; uncertainty  $\pm 0.12$  ppm). Projected CO<sub>2</sub> concentrations for five Shared Socio-economic Pathways (SSP) scenarios are indicated by dots on the right-hand side of each panel (grey background; (Meinshausen et al., 2020; SSPs are described in Section 1.6). **(b) Reconstruction of GMST from marine paleoclimate proxies** (light-grey line: Snyder (2016); dark grey line: Hansen et al. (2013); see Section 2.3.1 for an assessment). Observed and reconstructed temperature changes since 1850 are the AR6 assessed mean (referenced to 1850–1900; Box TS.3; 2.3.1.1); dots/whiskers on the right-hand panels (grey background) indicate the projected mean and ranges of warming derived from Coupled Model Intercomparison Project Phase 6 (CMIP6) SSP-based (2081–2100) and Model for the Assessment of Greenhouse Gas Induced Climate Change (MAGICC7; 2300) simulations (Tables 4.5 and 4.9). **(c) Sea level changes reconstructed from a stack of oxygen isotope measurements on seven ocean sediment cores** (Spratt and Lisiecki, 2016; see Chapter 2, Section 2.3.3.3 and Chapter 9, Section 9.6.2 for an assessment). The sea level record from 1850–1900 is from Kopp et al. (2016), while the 20th century record is an updated ensemble estimate of GMSL change (Palmer et al., 2021; Sections 2.3.3.3 and 9.6.1.1). Dots/whiskers on the right-hand panels of the figure (grey background) indicate the projected median and ranges derived from SSP-based simulations (2081–2100: Table 9.9; 2300: Section 9.6.3.5). Best estimates (dots) and uncertainties (whiskers), as assessed in Chapter 2, are included in the left and middle panels for each of the three indicators and selected paleo-reference periods used in this report (CO<sub>2</sub>: Table 2.1; GMST: Section 2.3.1.1 and Cross-Chapter Box 2.3, Table 1; GMSL: Sections 2.3.3.3 and 9.6.2. See also Cross-Chapter Box 2.1). Selected paleo-reference periods: LIG – Last Interglacial; LGM – Last Glacial Maximum; MH – mid-Holocene (Cross-Chapter Box 2.1, Table 1). The non-labelled best estimate in panel (c) corresponds to the sea level high-stand during Marine Isotope Stage 11, about 410 ka (410,000 years ago; Section 9.6.2). Further details on data sources and processing are available in the chapter data table (Table 1.SM.1).

IPCC 2021, Chap. 1



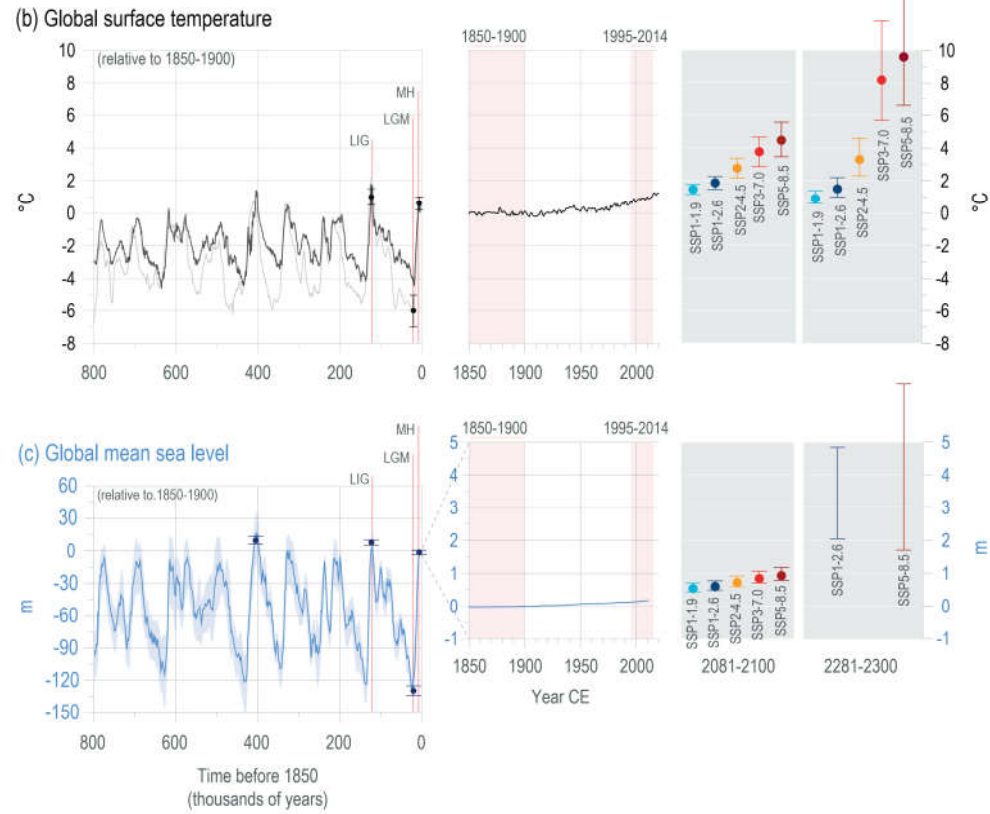
# Long-term context of anthropogenic climate change



IPCC 2021, Chap. 1



# Long-term context of anthropogenic climate change



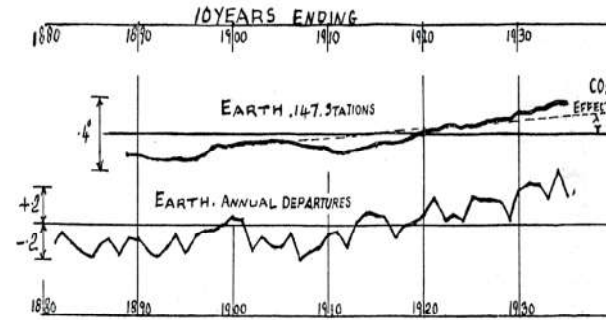
IPCC 2021, Chap. 1



# Callendar's estimates of global land temperature variations and their possible causes.

Changes in global land temperature (60°S–60°N) relative to a 1901–1930 baseline (°C)

(a) Callendar (1938)



(b) Comparing Callendar (1938, 1961) with CRUTEM5 (Osborn et al. 2021)

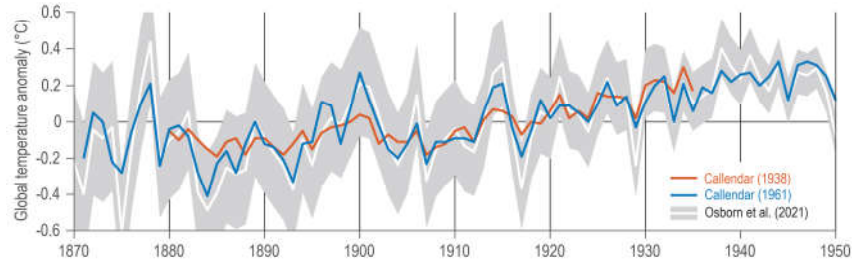


**Figure 1.8 | G.S. Callendar's estimates of global land temperature variations and their possible causes.** (a) The original figure from Callendar (1938), using measurements from 147 surface stations for 1880–1935, showing: (top) ten-year moving departures from the mean of 1901–1930 (°C), with the dashed line representing his estimate of the 'CO<sub>2</sub> effect' on temperature rise, and (bottom) annual departures from the 1901–1930 mean (°C). (b) Comparing the estimates of global land (60°S–60°N) temperatures tabulated in Callendar (1938, 1961) with a modern reconstruction (CRUTEM5, Osborn et al., 2021) for the same period, following Hawkins and Jones (2013). Further details on data sources and processing are available in the chapter data table (Table 1.SM.1).

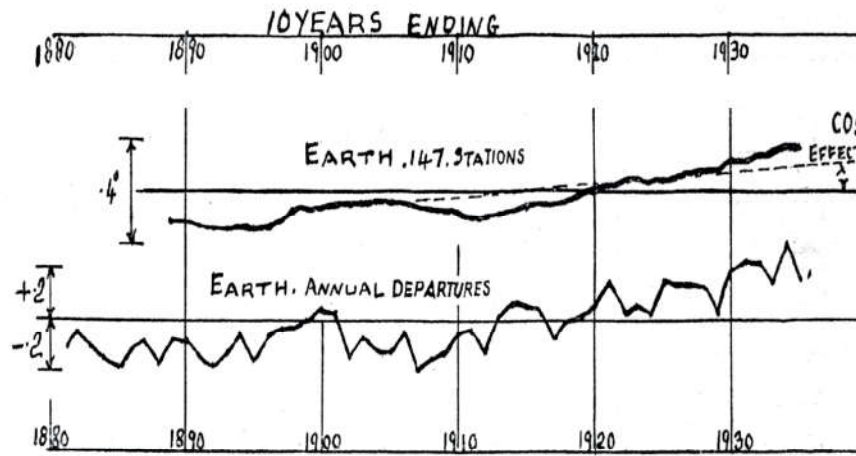




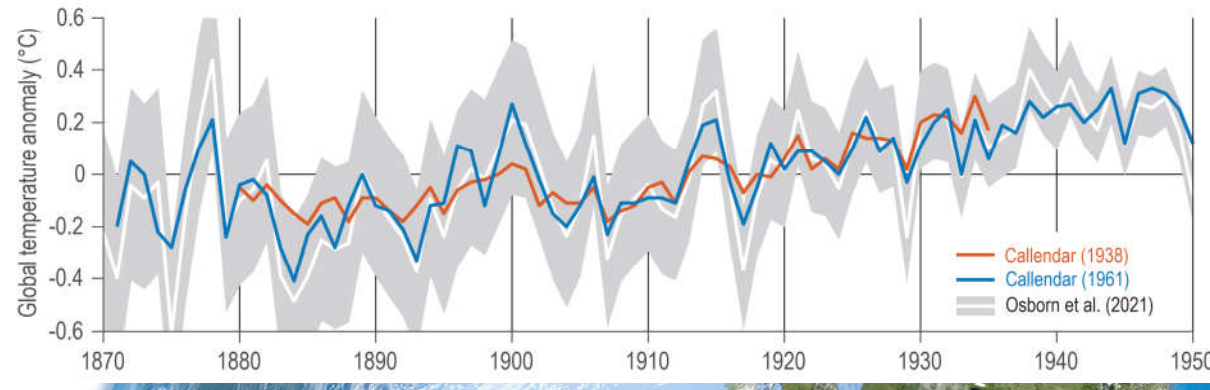
# Callendar's estimates of global land temperature variations and their possible causes.

Changes in global land temperature (60°S-60°N) relative to a 1901–1930 baseline (°C)

(a) Callendar (1938)



(b) Comparing Callendar (1938, 1961) with CRUTEM5 (Osborn et al. 2021)



# Range of projected temperature change for 1990–2030 for various regions defined in IPCC First Assessment Report (FAR)

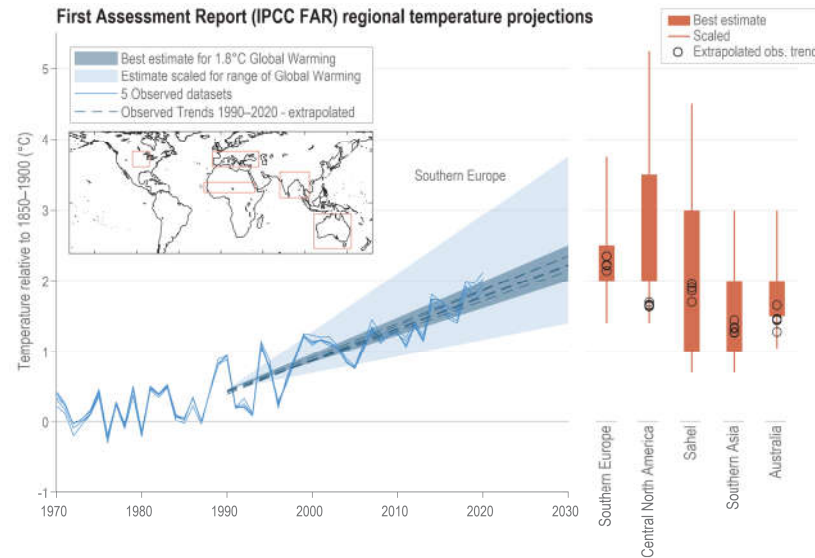
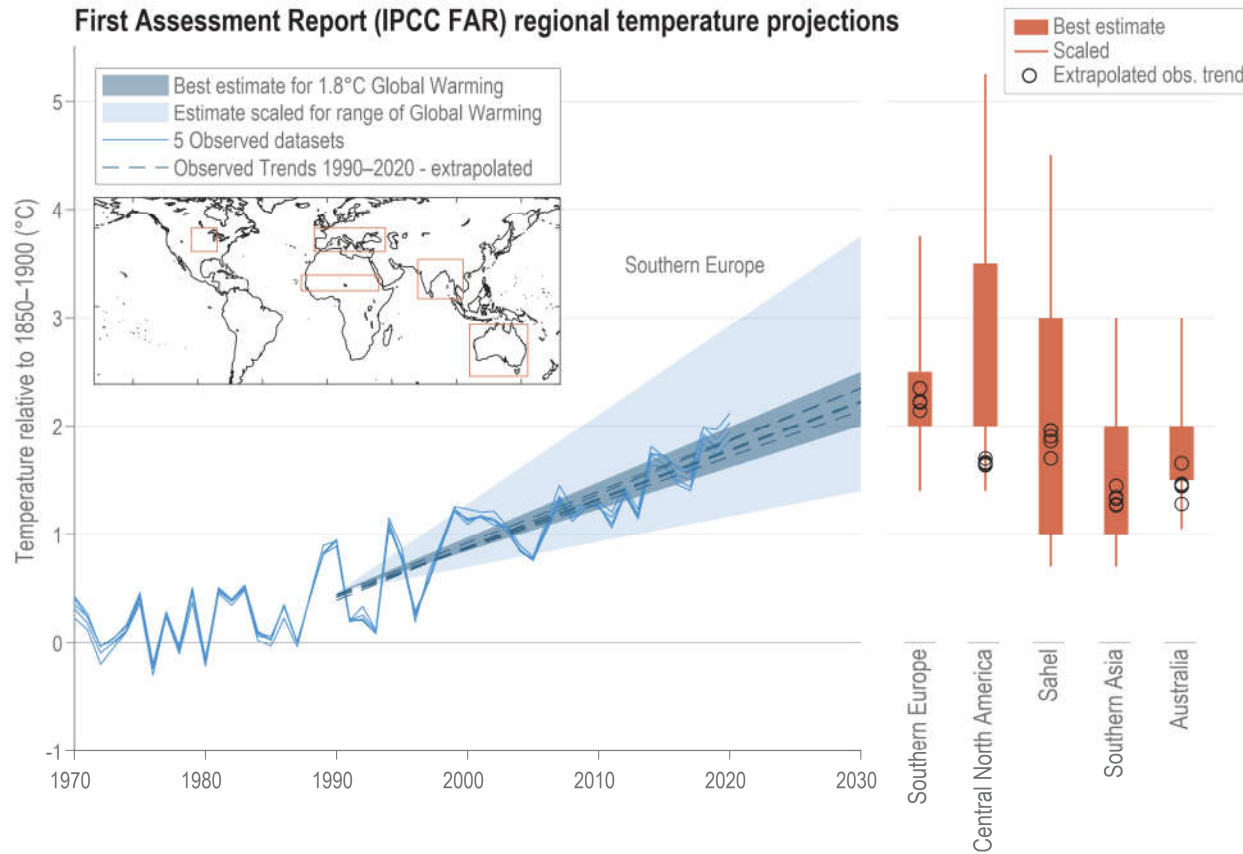
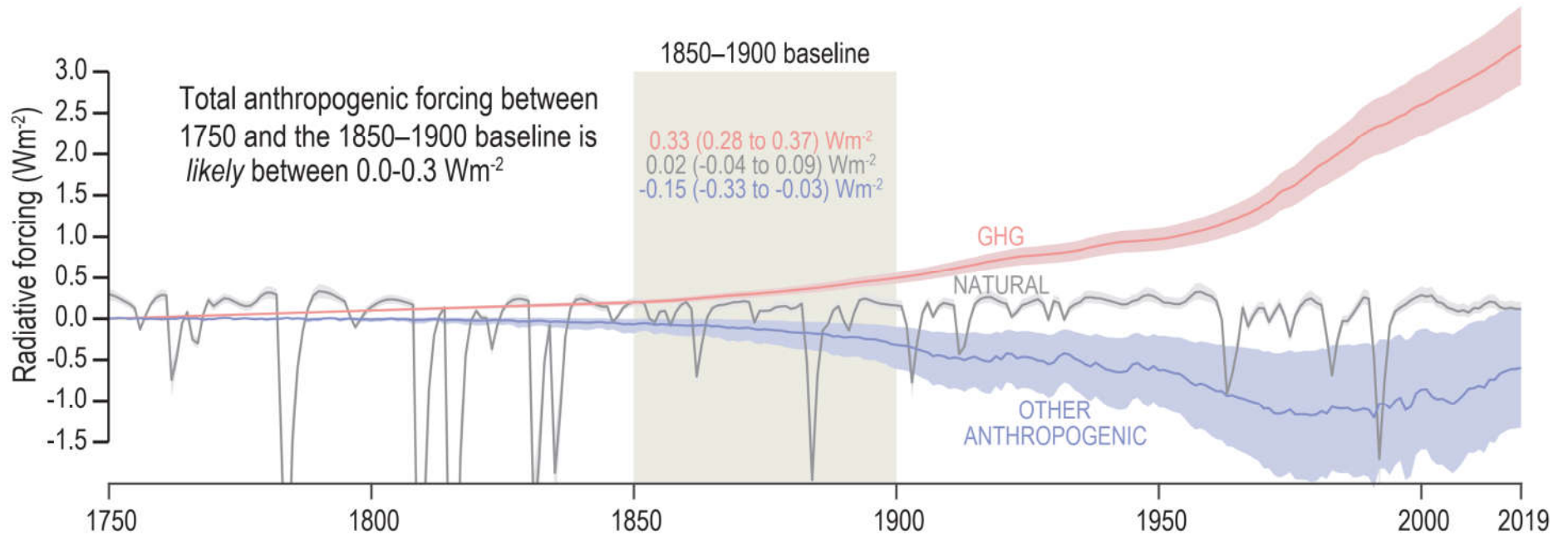


**Figure 1.10 | Range of projected temperature change for 1990–2030 for various regions defined in IPCC First Assessment Report (FAR).** The left-hand panel shows the FAR projections (IPCC, 1990a) for southern Europe, with the darker blue shade representing the range of projected change given for the best estimate of 1.8°C global warming by 2030 compared with pre-industrial levels, and the fainter blue shade showing the range scaled by –30% to +50% for lower and higher estimates of global warming. Blue lines show the regionally averaged observations from five global temperature gridded datasets, and blue dashed lines show the linear trends in those datasets for 1990–2020 extrapolated to 2030. Observed datasets are: HadCRUT5, Cowtan and Way, GISTEMP, Berkeley Earth and NOAA GlobalTemp. The inset map shows the definition of the FAR regions used. The right-hand panel shows projected temperature changes by 2030 for the various FAR regions, compared to the extrapolated observational trends, following Grose et al. (2017). Further details on data sources and processing are available in the chapter data table (Table 1.SM.1).

# Range of projected temperature change for 1990–2030 for various regions defined in IPCC First Assessment Report (FAR)



# Changes in radiative forcing from 1750 to 2019



**Cross-Chapter Box 1.2, Figure 1 | Changes in radiative forcing from 1750–2019.** The radiative forcing estimates from the AR6 emulator (Cross-Chapter Box 7.1) are split into GHG, other anthropogenic (mainly aerosols and land use) and natural forcings, with the average over the 1850–1900 baseline shown for each. Further details on data sources and processing are available in the chapter data table (Table 1.SM.1).

## Statements in the Executive Summary

### Framing and Context of the WGI Report (6)

**Natural climate variability can temporarily obscure or intensify anthropogenic climate change on decadal time scales, especially in regions with large internal interannual-to-decadal variability. At the current level of global warming, an observed signal of temperature change relative to the 1850–1900 baseline has emerged above the levels of background variability over virtually all land regions (*high confidence*).** Both the rate of long-term change and the amplitude of interannual (year-to-year) variability differ from global to regional to local scales, between regions and across climate variables, thus influencing when changes become apparent. Tropical regions have experienced less warming than most others, but also exhibit smaller interannual variations in temperature. Accordingly, the signal of change is more apparent in tropical regions than in regions with greater warming but larger interannual variations (*high confidence*). {1.4.2, FAQ1.2}



# Simulated changes in various climate indicators under historical and RCP4.5 scenarios using the MPI ESM Grand Ensemble

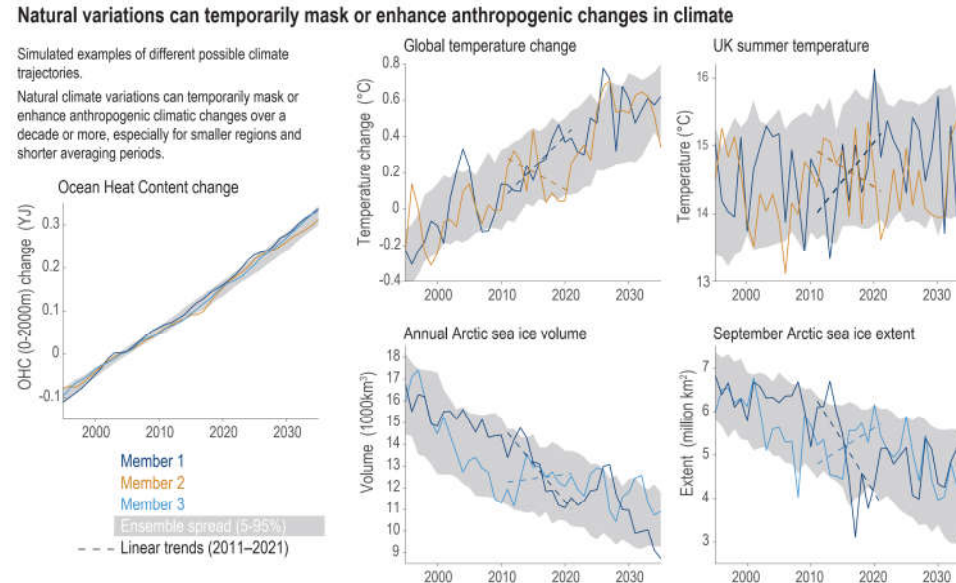


**Figure 1.13 | Simulated changes in various climate indicators under historical and RCP4.5 scenarios using the MPI ESM Grand Ensemble.** The grey shading shows the 5–95% range from the 100-member ensemble. The coloured lines represent individual example ensemble members, with linear trends for the 2011–2021 period indicated by the dashed lines. Changes in ocean heat content (OHC) over the top 2000 m represents the integrated signal of global warming (**left**). The **top row** shows surface air temperature-related indicators (annual GSAT change and UK summer temperatures) and the **bottom row** shows Arctic sea ice-related indicators (annual ice volume and September sea ice extent). For smaller regions and for shorter time-period averages the variability increases and simulated short-term trends can temporarily mask or enhance anthropogenic changes in climate. Data from Maher et al. (2019). Further details on data sources and processing are available in the chapter data table (Table 1.SM.1).

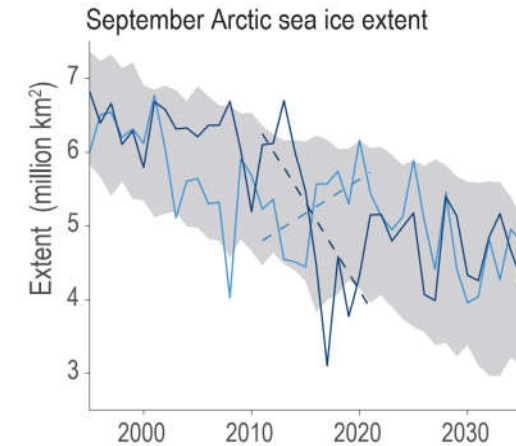
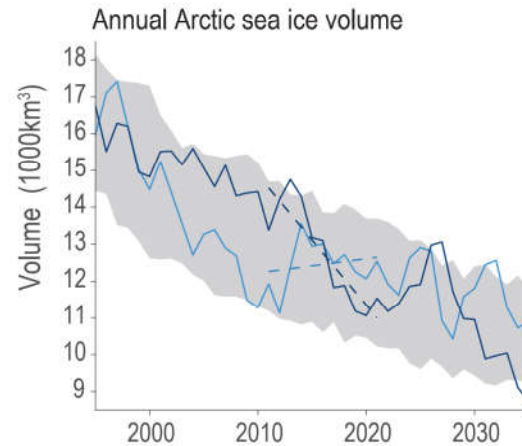
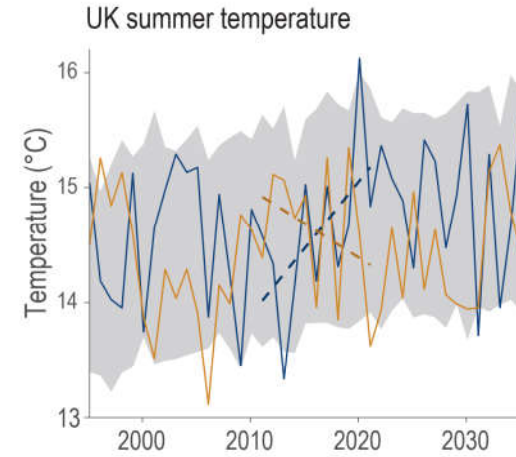
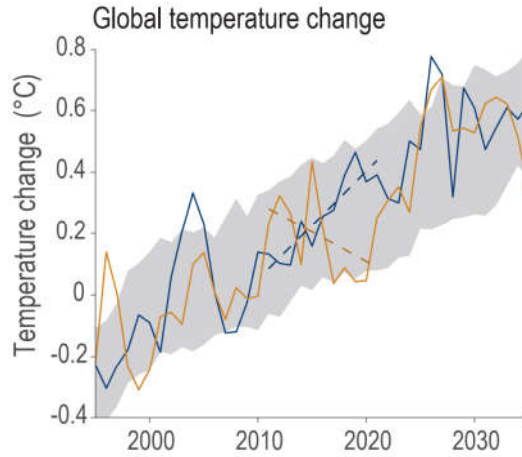
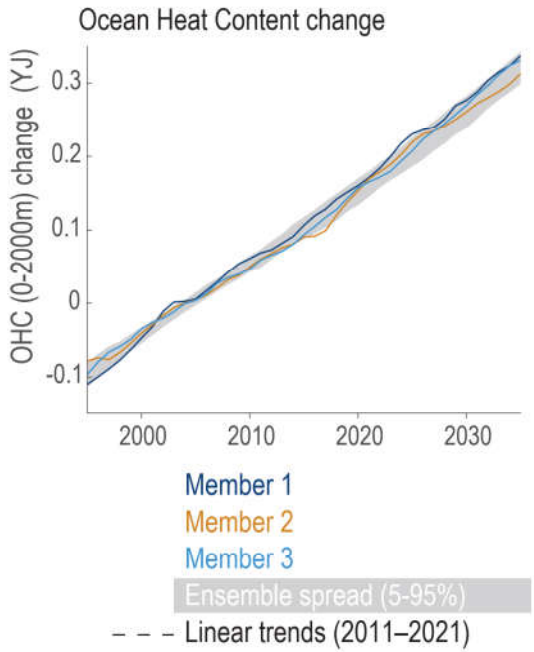




## Natural variations can temporarily mask or enhance anthropogenic changes in climate

Simulated examples of different possible climate trajectories.

Natural climate variations can temporarily mask or enhance anthropogenic climatic changes over a decade or more, especially for smaller regions and shorter averaging periods.





# Simulated changes in various climate indicators under historical and RCP4.5 scenarios using the MPI ESM Grand Ensemble

## Natural variations can temporarily obscure or intensify anthropogenic changes in climate

Simulated examples of different possible climate trajectories.

Natural climate variations can temporarily obscure or intensify anthropogenic climatic changes over a decade or more, especially for smaller regions and shorter averaging periods.

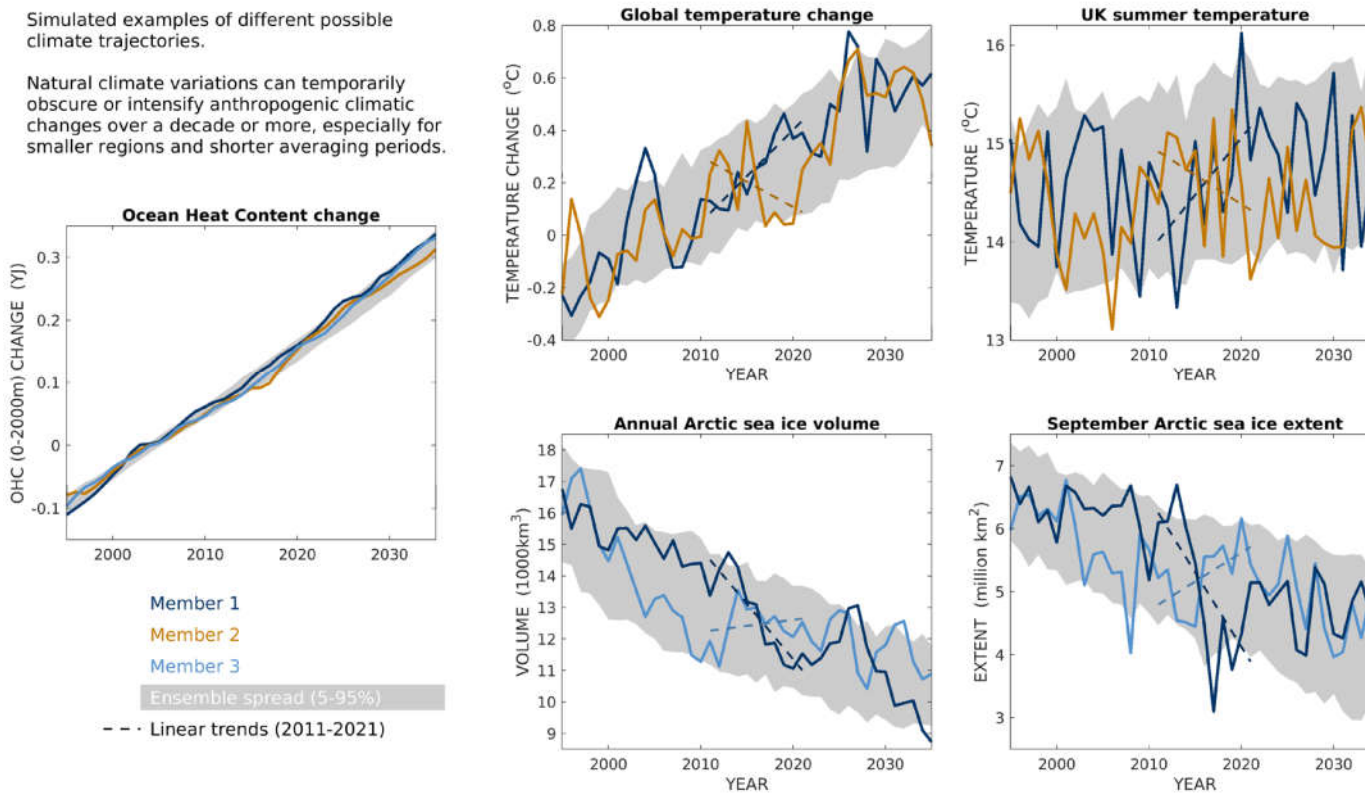


**Figure 1.13: Simulated changes in various climate indicators under historical and RCP4.5 scenarios using the MPI ESM Grand Ensemble.** The grey shading shows the 5–95% range from the 100-member ensemble. The coloured lines represent individual example ensemble members, with linear trends for the 2011–2021 period indicated by the thin dashed lines. Changes in Ocean Heat Content (OHC) over the top 2000m represents the integrated signal of global warming (left). The top row shows surface air temperature-related indicators (annual GSAT change and UK summer temperatures) and the bottom row shows Arctic sea-ice related indicators (annual ice volume and September sea ice extent). For smaller regions and for shorter time period averages the variability increases and simulated short-term trends can temporarily obscure or intensify anthropogenic changes in climate. Data from Maher et al., (2019). Further details on data sources and processing are available in the chapter data table (Table 1.SM.1).





## Changes in tropopause height and surface temperature

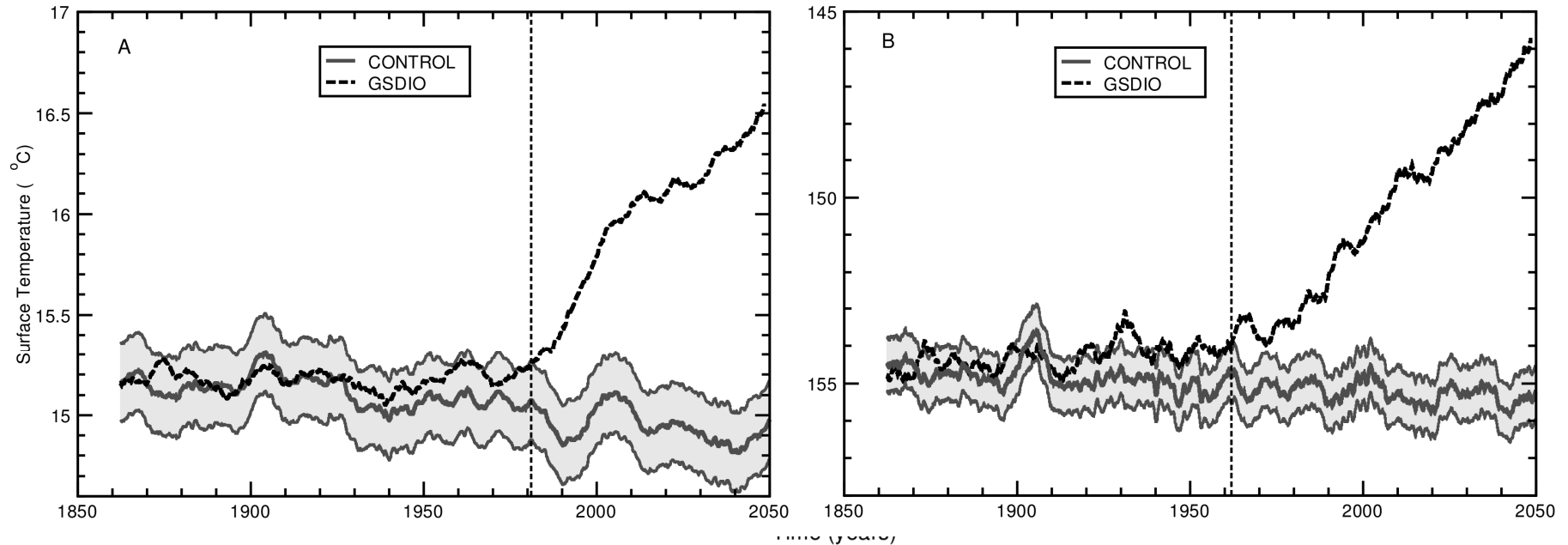


**Figure 3:** Filtered global-mean monthly-mean near-surface temperature (panel A) and  $p_{LRT}$  (panel B) in the ECHAM GSDIO and control simulations. Data were smoothed with a 60-month moving average window; bold lines are the filtered values. The grey envelope denotes the  $\pm 2\sigma$  ‘noise envelope’ in the control run data. Dashed vertical lines indicate the times at which the GSDIO surface temperature and  $p_{LRT}$  data separate from (and remain outside) the noise envelope. For display purposes, only the first 191 years of the 300-year control run are shown.

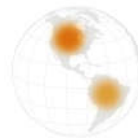
*Sausen and Santer, 2003*



# Observed variations in regional temperatures since 1850

## FAQ 1.2: Where is climate change most apparent?

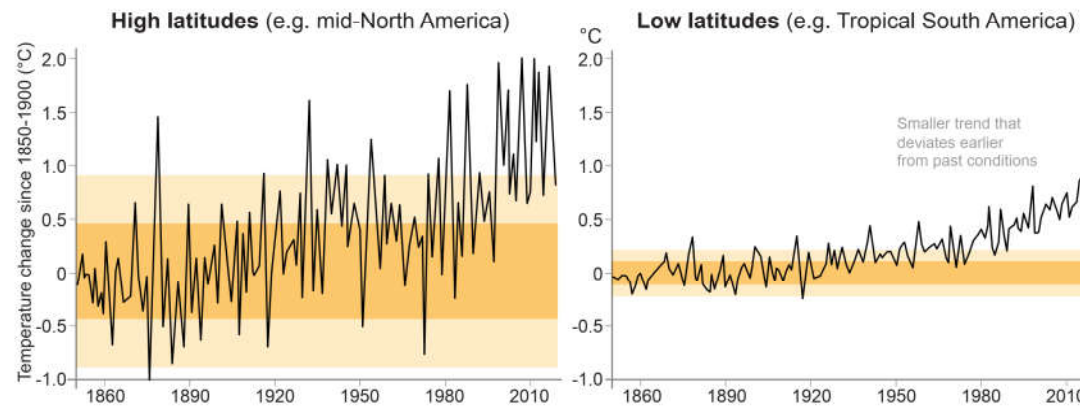
Temperature changes are most apparent in regions with smaller natural variations.



Estimation of:

2 standard deviations of natural year-to-year variations

1 standard deviation of natural year-to-year variations

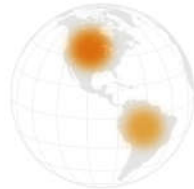


**FAQ 1.2, Figure 1 | Observed variations in regional temperatures since 1850 (data from Berkeley Earth).** Regions in high latitudes, such as mid-North America (40°N–64°N, 140°W–60°W, **left**), have warmed by a larger amount than regions at lower latitudes, such as tropical South America (10°S–10°N, 84°W–16°W, **right**), but the natural variations are also much larger at high latitudes (darker and lighter shading represents 1 and 2 standard deviations, respectively, of natural year-to-year variations). The signal of observed temperature change emerged earlier in tropical South America than mid-North America even though the changes were of a smaller magnitude. (Note that those regions were chosen because of the longer length of their observational record; see Figure 1.14 for more regions).

# Observed variations in regional temperatures since 1850

## FAQ 1.2: Where is climate change most apparent?

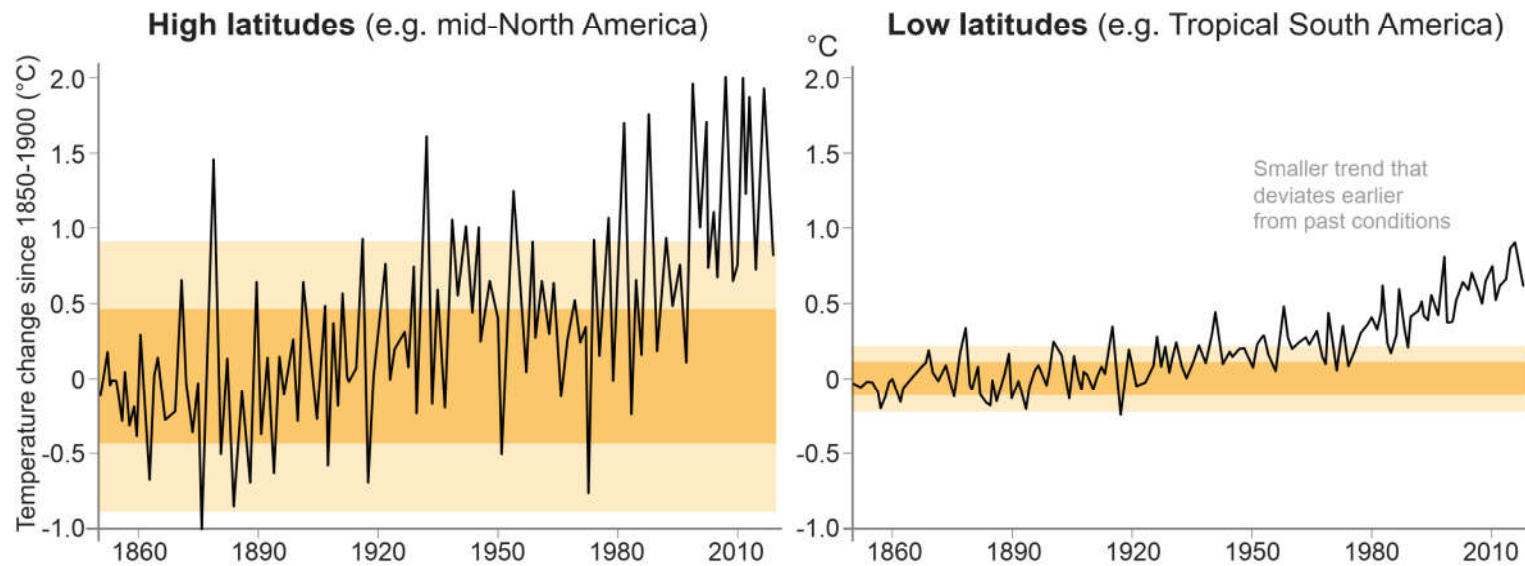
Temperature changes are most apparent in regions with smaller natural variations.



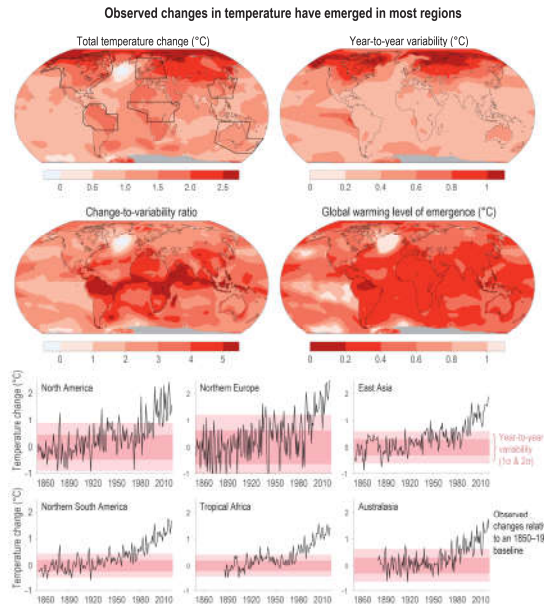
Estimation of:

2 standard deviations of natural year-to-year variations

1 standard deviation of natural year-to-year variations

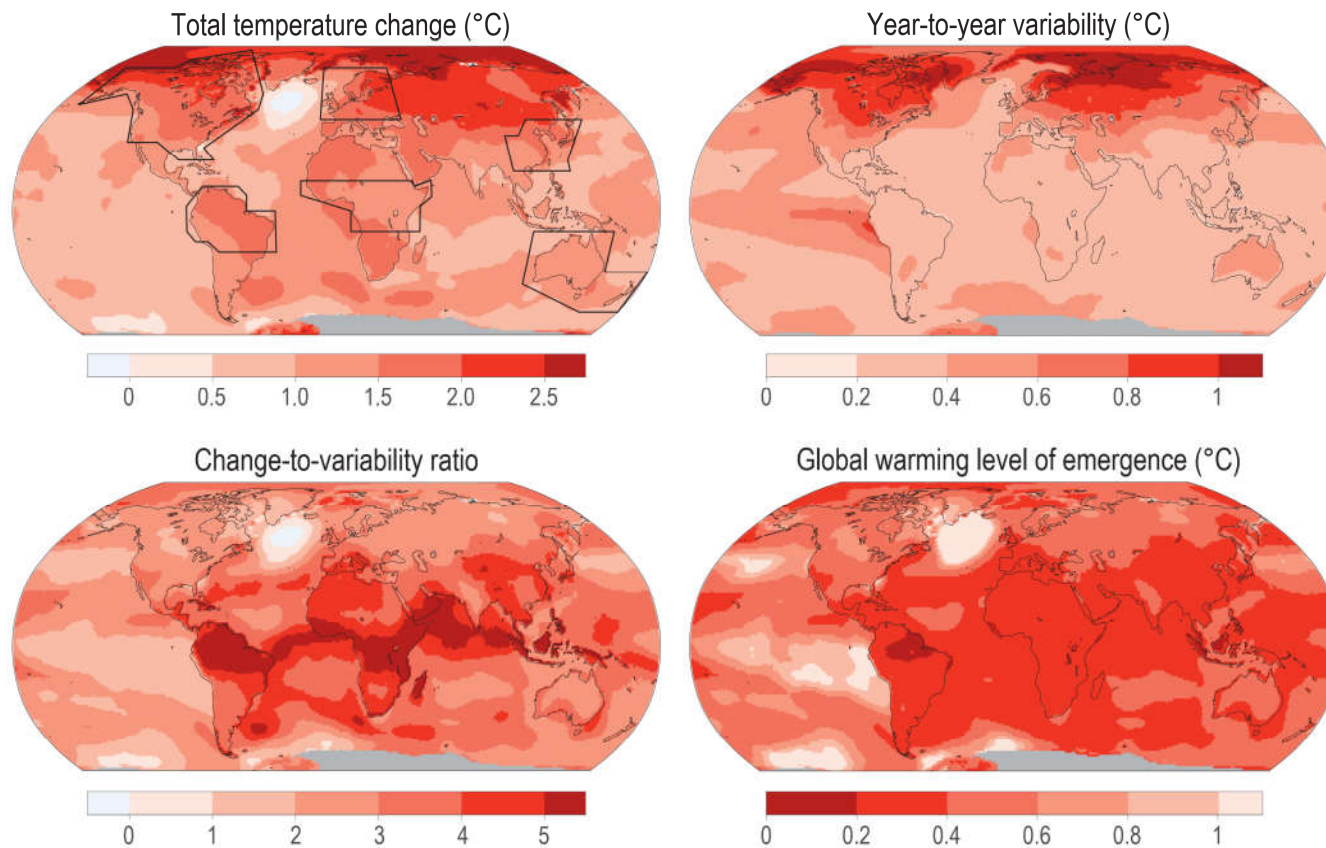


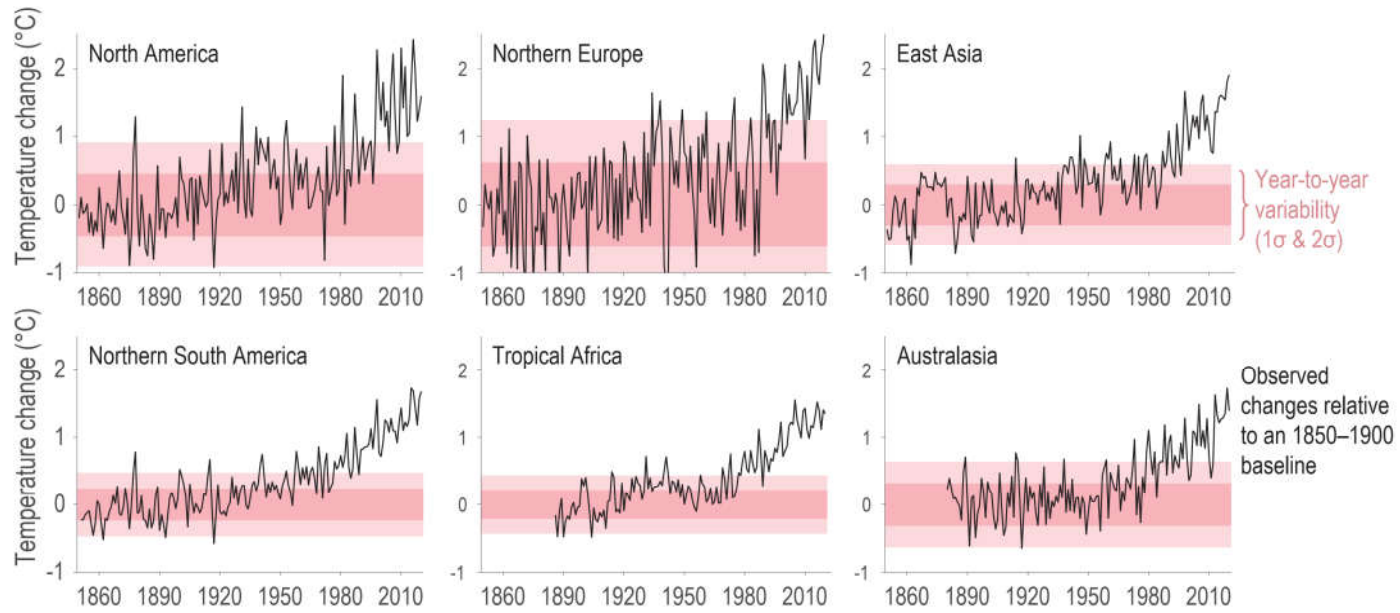
## The observed emergence of changes in temperature.



**Figure 1.14 | The observed emergence of changes in temperature.** (Top left) The total change in temperature estimated for 2020 relative to 1850–1900 (following Hawkins et al., 2020), showing the largest warming occurring in the Arctic. (Top right) The amplitude of estimated year-to-year variations in temperature. (Middle left) The ratio of the observed total change in temperature and the amplitude of temperature variability (the ‘signal-to-noise (S/N) ratio’), showing that the warming is most apparent in the tropical regions (also see FAQ 1.2). (Middle right) The global warming level at which the change in local temperature becomes larger than the local year-to-year variability. The **bottom** panels show time series of observed annual mean surface air temperatures over land in various example regions, as indicated by the boxes in the top-left panel. The 1 and 2 standard deviations ( $\sigma$ ) of estimated year-to-year variations for that region are shown by the pink shaded bands. Observed temperature data from Berkeley Earth (Rohde and Hausfather, 2020). Further details on data sources and processing are available in the chapter data table (Table 1.SM.1).

## Observed changes in temperature have emerged in most regions





# The 'cascade of uncertainties' in CMIP6 projections

Cascade of uncertainties in climate projections

Different sources of uncertainty dominate the total uncertainty in projections for different variables, regions and time periods

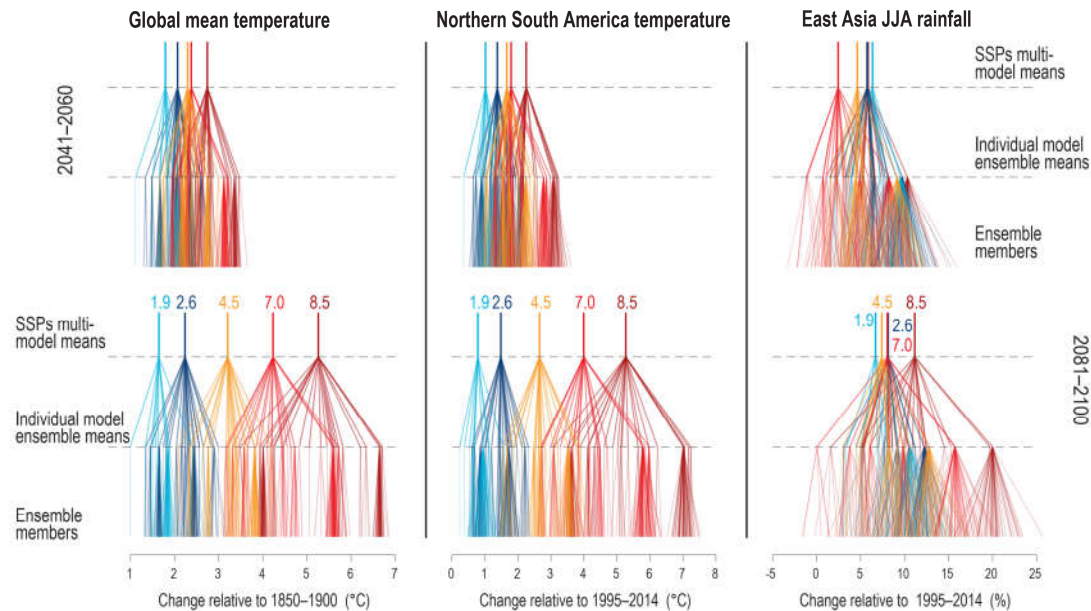
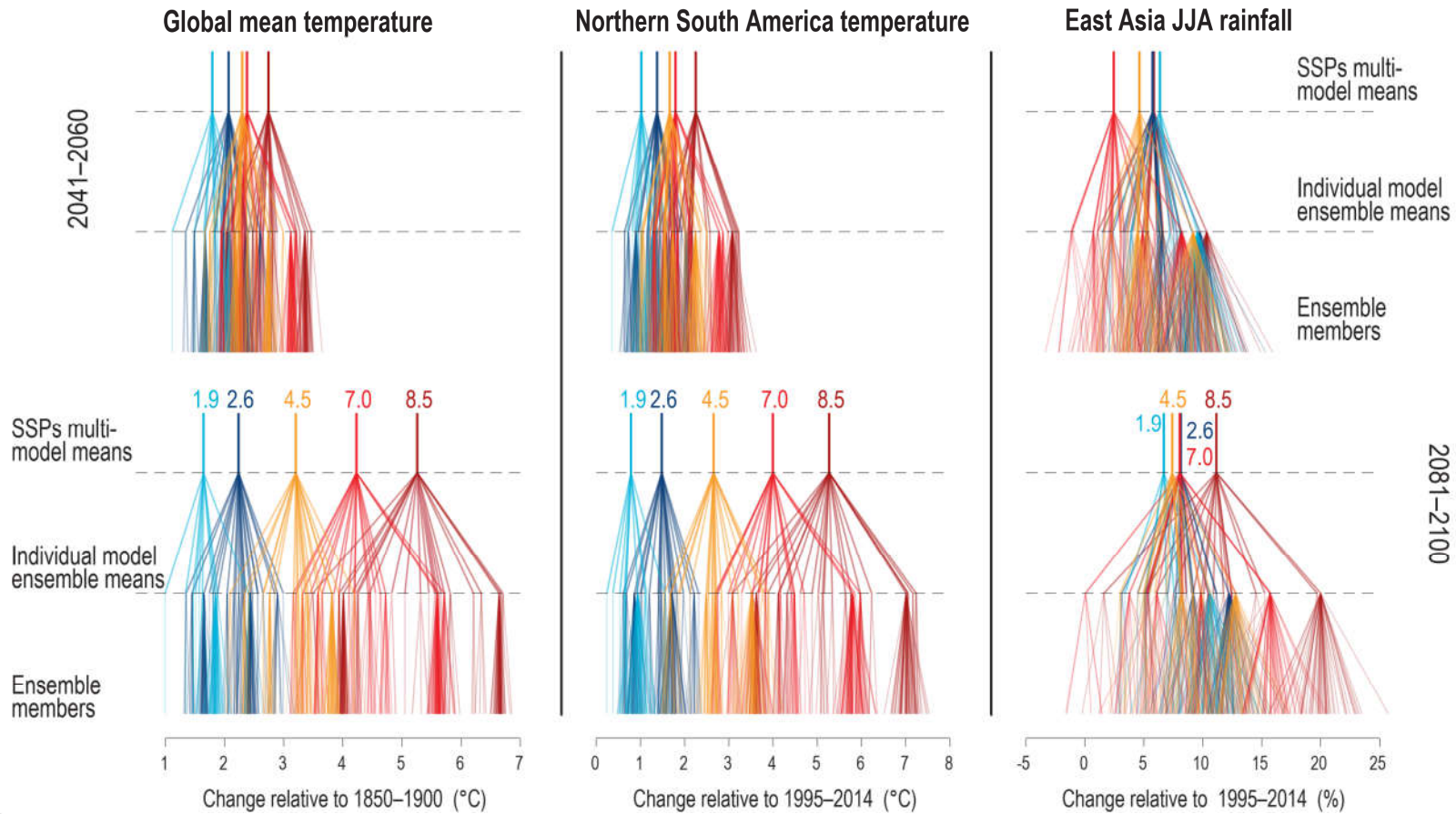


**Figure 1.15 | The 'cascade of uncertainties' in CMIP6 projections.** Changes in: GSAT (**left**); Northern South America temperature (**middle**); and East Asia summer (June–July–August, JJA) precipitation (**right**). These are shown for two time periods: 2041–2060 (**top**) and 2081–2100 (**bottom**). The SSP–radiative forcing combination is indicated at the top of each cascade at the value of the multi-model mean for each scenario. This branches downwards to show the ensemble mean for each model, and further branches into the individual ensemble members, although often only a single member is available. These diagrams highlight the relative importance of different sources of uncertainty in climate projections, which varies for different time periods, regions and climate variables. See Section 1.4.5 for the definition of the regions used. Further details on data sources and processing are available in the chapter data table (Table 1.SM.1).

# Cascade of uncertainties in climate projections

Different sources of uncertainty dominate the total uncertainty in projections for different variables, regions and time periods



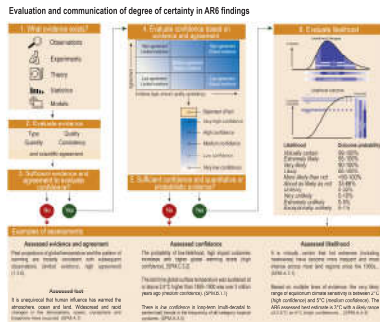


# Statements in the Executive Summary

## Framing and Context of the WGI Report (7)

**The AR6 has adopted a unified framework of climate risk, supported by an increased focus in WGI on low-likelihood, high-impact events.** Systematic risk framing is intended to aid the formulation of effective responses to the challenges posed by current and future climatic changes and to better inform risk assessment and decision-making. AR6 also makes use of the 'storylines' approach, which contributes to building a robust and comprehensive picture of climate information, allows a more flexible consideration and communication of risk, and can explicitly address low-likelihood, high-impact events. {1.1.2, 1.4.4, Cross-Chapter Box 1.3}





#### 4. Evaluate confidence based on evidence and agreement

Agreement ↑	High agreement Limited evidence	High agreement Robust evidence
	Medium agreement Medium evidence	
	Low agreement Limited evidence	Low agreement Robust evidence

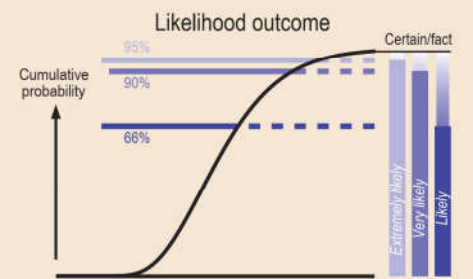
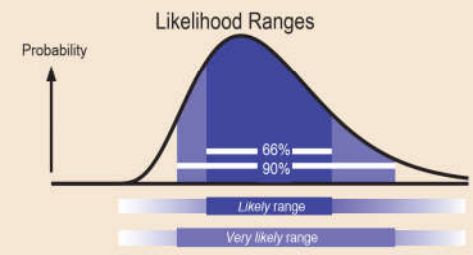
Evidence (type, amount, quality, consistency) →

- Statement of fact
- Very high confidence
- High confidence
- Medium confidence
- Low confidence
- Very low confidence

#### 5. Sufficient confidence and quantitative or probabilistic evidence?



#### 6. Evaluate likelihood



Likelihood	Outcome probability
Virtually certain	99-100%
Extremely likely	95-100%
Very likely	90-100%
Likely	66-100%
More likely than not	>50-100%
About as likely as not	33-66%
Unlikely	0-33%
Very unlikely	0-10%
Extremely unlikely	0-5%
Exceptionally unlikely	0-1%

# Illustrating concepts of low-likelihood scenarios

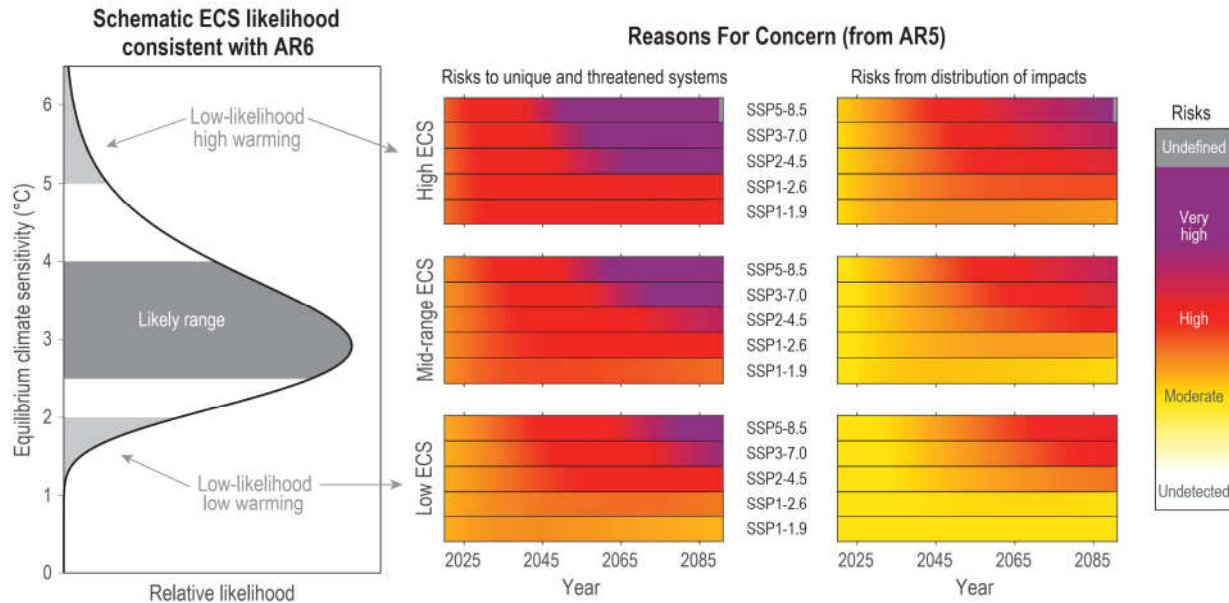
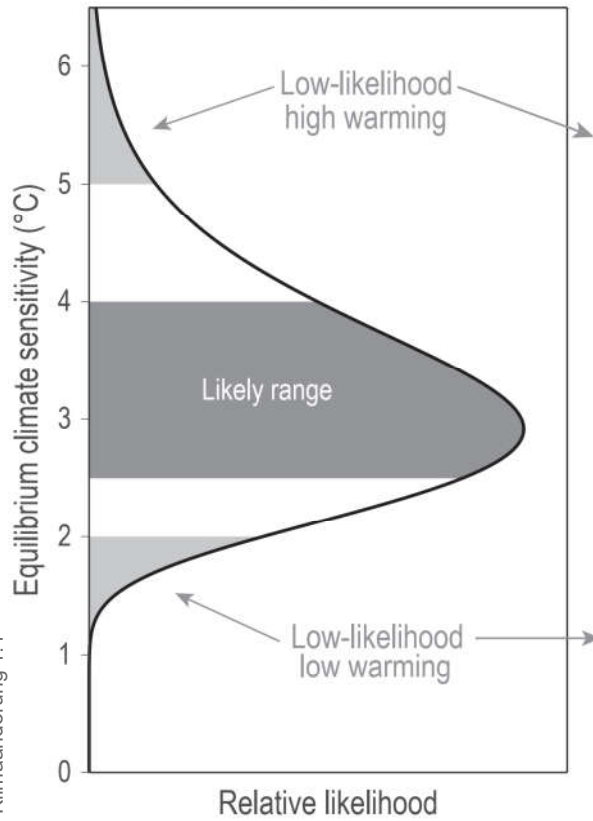


**Figure 1.16 | Illustrating concepts of low-likelihood outcomes.** **Left:** schematic likelihood distribution consistent with the IPCC AR6 assessments that equilibrium climate sensitivity (ECS) is *likely* in the range 2.5°C to 4.0°C, and *very likely* between 2.0°C and 5.0°C (Chapter 7). ECS values outside the assessed *very likely* range are designated low-likelihood outcomes in this example (light grey). **Middle and right-hand columns:** additional risks due to climate change for 2020–2090 using the Reasons For Concern (RFCs, see IPCC, 2014b), specifically RFC1 describing the risks to unique and threatened systems and RFC3 describing risks from the distribution of impacts (O’Neill et al., 2017b; Zommers et al., 2020). The projected changes of GSAT used are the 95%, median and 5% assessed ranges from Chapter 4 for each SSP (top, middle and bottom); these are designated High ECS, Mid-range ECS and Low ECS respectively. The ‘burning-ember’ risk spectrum of graduated colours is usually associated with levels of committed GSAT change; instead, this illustration associates the risk spectrum with the GSAT temperature reached in each year from 2020 to 2090. Note that this illustration does not include the vulnerability aspect of each SSP scenario. Further details on data sources and processing are available in the chapter data table (Table 1.SM.1).

### Schematic ECS likelihood consistent with AR6



### Reasons For Concern (from AR5)

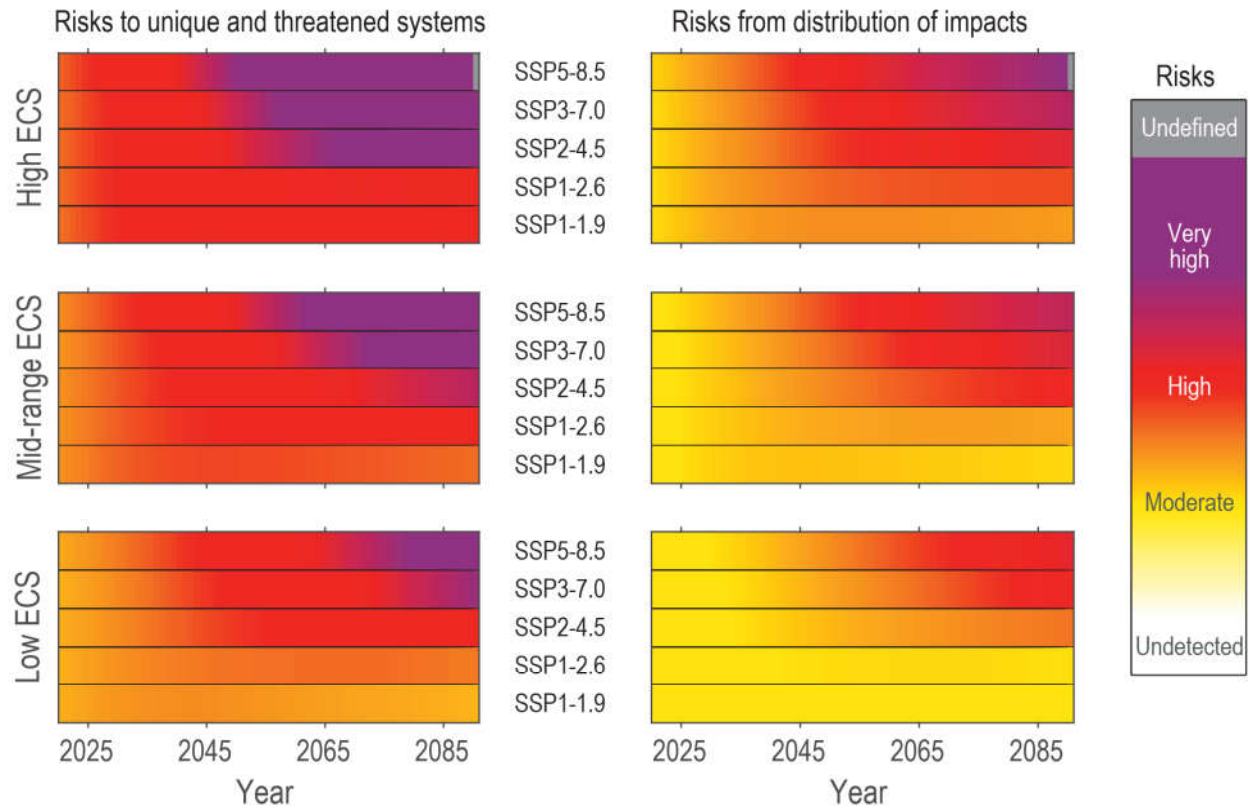


## Illustration of two types of tipping points: noise-induced and bifurcation

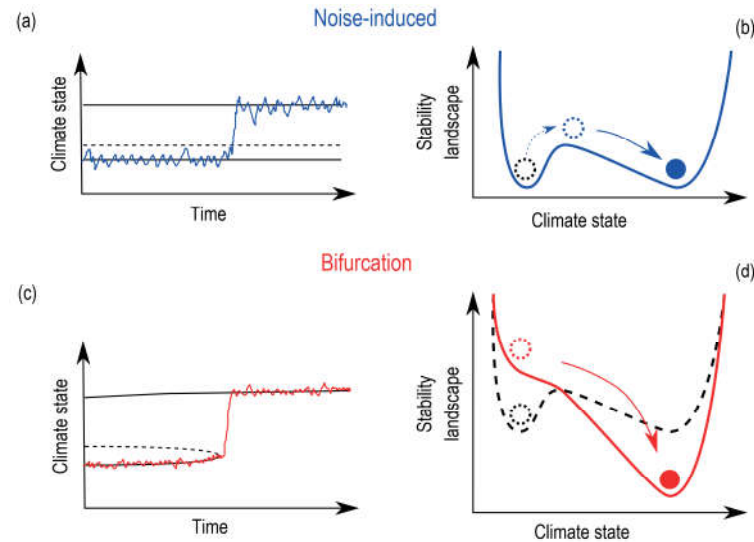
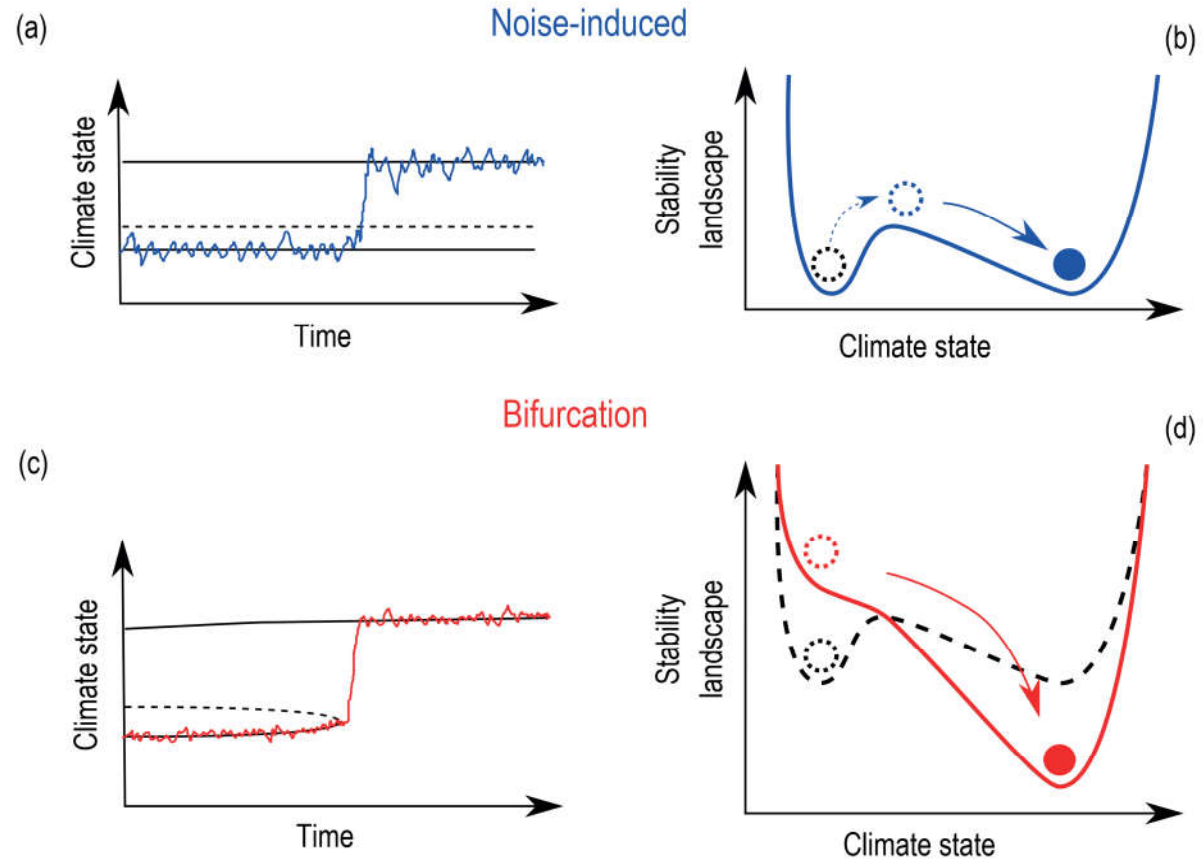


**Figure 1.17 | Illustration of two types of tipping points: noise-induced (a, b) and bifurcation (c, d).** (a) and (c) are example time-series (coloured lines) through the tipping point, with solid-black lines indicating stable climate states (e.g., low or high rainfall) and dashed lines representing the boundary between stable states. (b) and (d) are stability landscapes, which provide an intuitive understanding of the different types of tipping point. The 'valleys' represent different climate states the system can occupy, with 'hilltops' separating the stable states. The resilience of a climate state is implied by the depth of the valley. The current state of the system is represented by a ball. Both scenarios assume that the ball starts in the left-hand valley (dashed-black lines) and then through different mechanisms dependent on the type of tipping transitions to the right-hand valley (coloured lines). Noise-induced tipping events (a, b), for instance drought events causing sudden dieback of the Amazon rainforest, develop from fluctuations within the system. The stability landscape in this scenario remains fixed and stationary. A series of perturbations in the same direction, or one large perturbation, are required to force the system over the hilltop and into the alternative stable state. Bifurcation tipping events (c, d), such as a collapse of the thermohaline circulation in the Atlantic Ocean under climate change, occur when a critical level in the forcing is reached. Here the stability landscape is subjected to a change in shape. Under gradual anthropogenic forcing the left-hand valley begins to shallow and eventually vanishes at the tipping point, forcing the system to transition to the right-hand valley.



# Statements in the Executive Summary

## Framing and Context of the WGI Report (8)

**The construction of climate change information and communication of scientific understanding are influenced by the values of the producers, the users and their broader audiences.** Scientific knowledge interacts with pre-existing conceptions of weather and climate, including values and beliefs stemming from ethnic or national identity, traditions, religion or lived relationships to land and sea (*high confidence*). Science has values of its own, including objectivity, openness and evidence-based thinking. Social values may guide certain choices made during the construction, assessment and communication of information (*high confidence*). {1.2.3, Box 1.1}



# Choice of baseline matters when comparing observations and model simulations

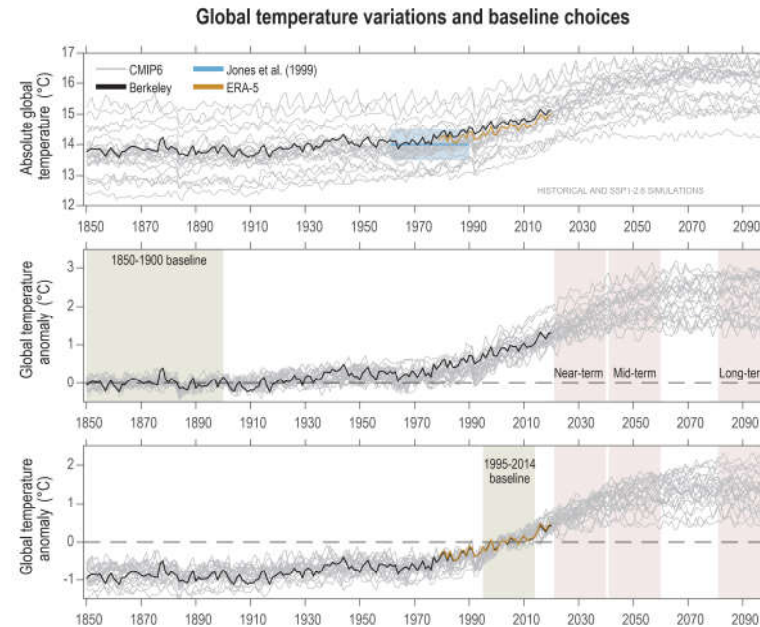
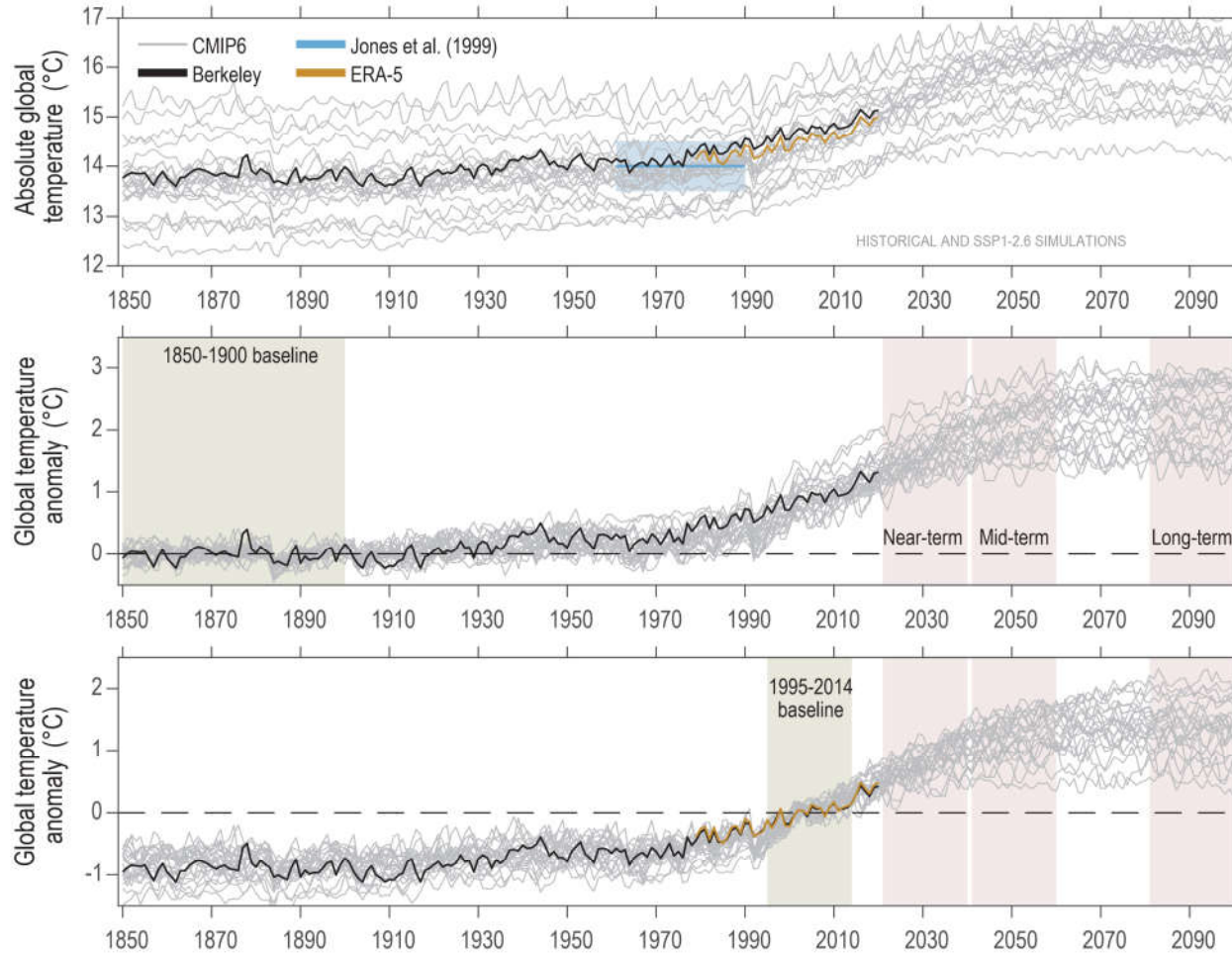


**Figure 1.11 | Choice of baseline matters when comparing observations and model simulations.** Global mean surface air temperature (GSAT, grey) from a range of CMIP6 historical simulations (1850–2014; 25 models) and SSP1-2.6 (2015–2100) using absolute values (**top**) and anomalies relative to two different baselines: 1850–1900 (**middle**) and 1995–2014 (**bottom**). An estimate of GSAT from a reanalysis (ERA-5, orange, 1979–2020) and an observation-based estimate of global mean surface air temperature (GMST) (Berkeley Earth, black, 1850–2020) are shown, along with the mean GSAT for 1961–1990 estimated by Jones et al. (1999), light blue shading ( $14.0^{\circ}\text{C} \pm 0.5^{\circ}\text{C}$ ). Using the more recent baseline (bottom) allows the inclusion of datasets which do not include the periods of older baselines. The middle and bottom panels have scales which are the same size but offset. Further details on data sources and processing are available in the chapter data table (Table 1.SM.1).





### Global temperature variations and baseline choices



## Statements in the Executive Summary

### Data, Tools and Methods Used across the WGI Report (1)

**Capabilities for observing the physical climate system have continued to improve and expand overall, but some reductions in observational capacity are also evident (*high confidence*).** Improvements are particularly evident in ocean observing networks and remote-sensing systems, and in paleoclimate reconstructions from proxy archives. However, some climate-relevant observations have been interrupted by the discontinuation of surface stations and radiosonde launches, and delays in the digitisation of records. Further reductions are expected to result from the COVID-19 pandemic. In addition, paleoclimate archives such as mid-latitude and tropical glaciers as well as modern natural archives used for calibration (e.g., corals and trees) are rapidly disappearing owing to a host of pressures, including increasing temperatures (*high confidence*). {1.5.1}



# Temporal coverage of selected instrumental climate observations (top) and selected paleoclimate archives (bottom)

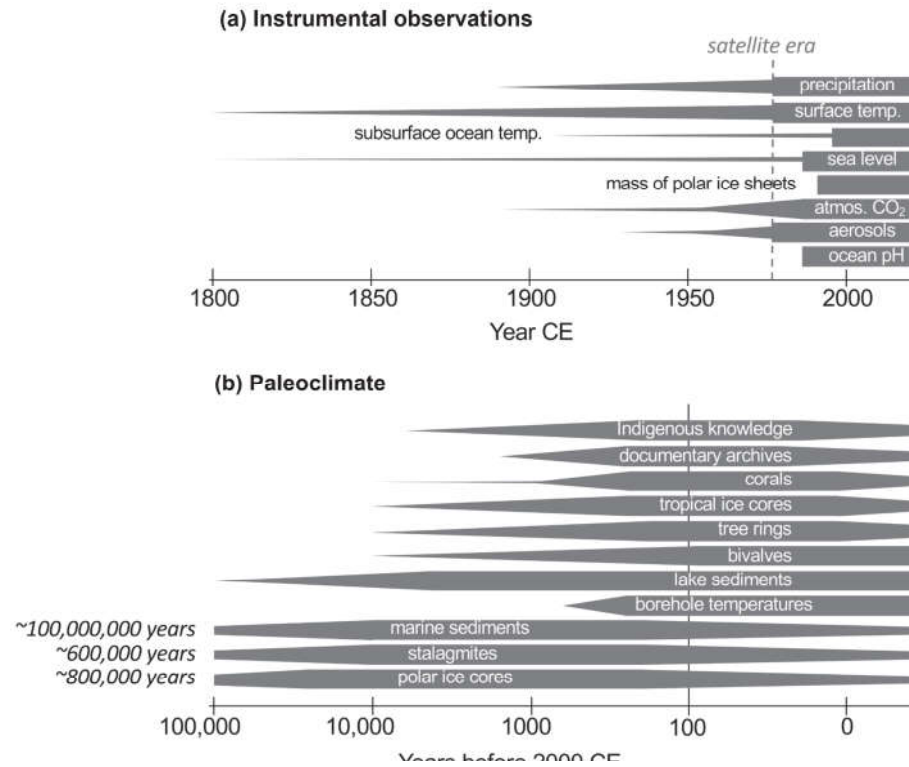
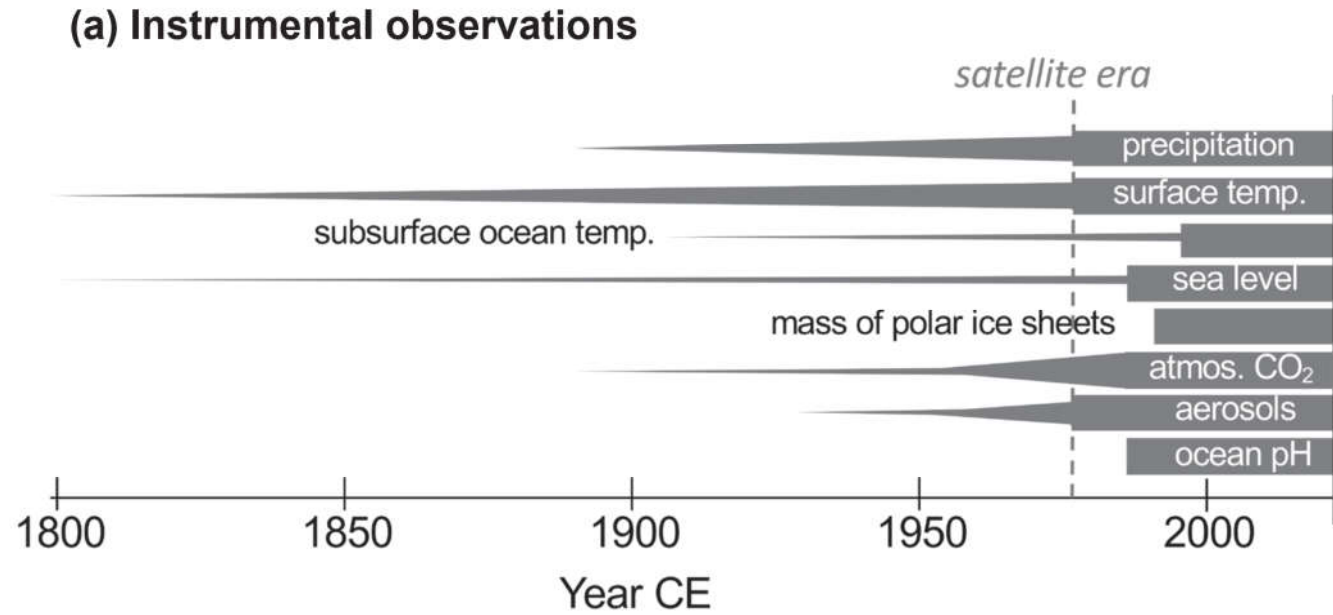
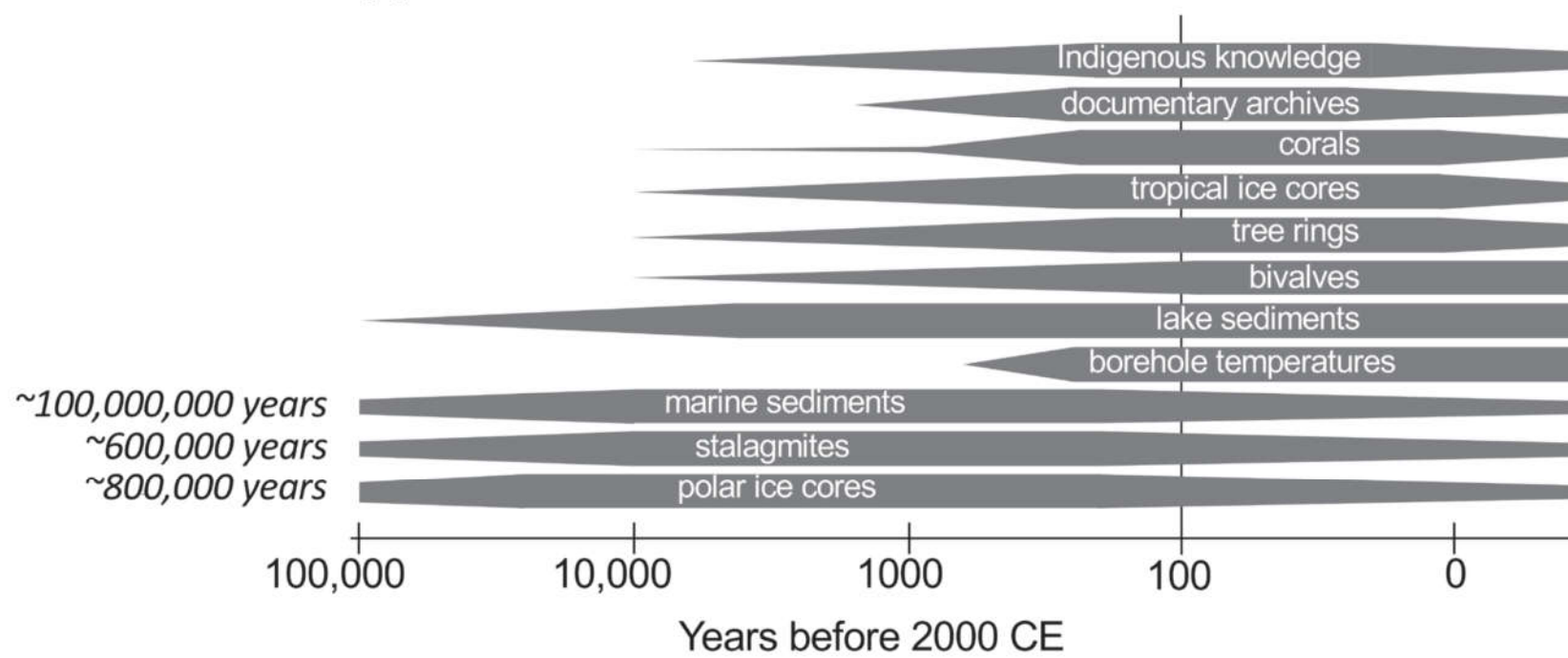


**Figure 1.7 | Schematic of temporal coverage of (a) selected instrumental climate observations and (b) selected paleoclimate archives.** The satellite era began in 1979 CE. The width of the taper gives an indication of the amount of available records.





## (b) Paleoclimate



IPCC 2021, Chap. 1



## Statements in the Executive Summary

### Data, Tools and Methods Used across the WGI Report (2)

**Reanalyses have improved since AR5 and are increasingly used as a line of evidence in assessments of the state and evolution of the climate system (*high confidence*).**

Reanalyses, where atmosphere or ocean forecast models are constrained by historical observational data to create a climate record of the past, provide consistency across multiple physical quantities and information about variables and locations that are not directly observed. Since AR5, new reanalyses have been developed with various combinations of increased resolution, extended records, more consistent data assimilation, estimation of uncertainty arising from the range of initial conditions, and an improved representation of the ocean. While noting their remaining limitations, the WGI report uses the most recent generation of reanalysis products alongside more standard observation-based datasets.

{1.5.2, Annex 1}



## Statements in the Executive Summary

### Data, Tools and Methods Used across the WGI Report (3)

**Since AR5, new techniques have provided greater confidence in attributing changes in climate extremes to climate change.** Attribution is the process of evaluating the relative contributions of multiple causal factors to an observed change or event. This includes the attribution of the causal factors of changes in physical or biogeochemical weather or climate variables (e.g., temperature or atmospheric CO<sub>2</sub>) as done in, or of the impacts of these changes on natural and human systems (e.g., infrastructure damage or agricultural productivity), as done in WGII. Attributed causes include human activities (such as emissions of greenhouse gases and aerosols, or land-use change), and changes in other aspects of the climate, or natural or human systems. {Cross-WG Box 1.1}



## Statements in the Executive Summary

### Data, Tools and Methods Used across the WGI Report (4)

The latest generation of complex climate models has an improved representation of physical processes, and a wider range of Earth system models now represent biogeochemical cycles. Since the AR5, higher-resolution models that better capture smaller-scale processes and extreme events have become available. Key model intercomparisons supporting this assessment include the Coupled Model Intercomparison Project Phase 6 (CMIP6) and the Coordinated Regional Climate Downscaling Experiment (CORDEX), for global and regional models respectively. Results using CMIP Phase 5 (CMIP5) simulations are also assessed. Since the AR5, large ensemble simulations, where individual models perform multiple simulations with the same climate forcings, are increasingly used to inform understanding of the relative roles of internal variability and forced change in the climate system, especially on regional scales. The broader availability of ensemble model simulations has contributed to better estimations of uncertainty in projections of future change (*high confidence*). A broad set of simplified climate models is assessed and used as emulators to transfer climate information across research communities, such as for evaluating impacts or mitigation pathways consistent with certain levels of future warming. {1.4.2, 1.5.3, 1.5.4, Cross-chapter Box 30 7.1}



## A world map showing the increased diversity of modelling centres contributing to CMIP and CORDEX

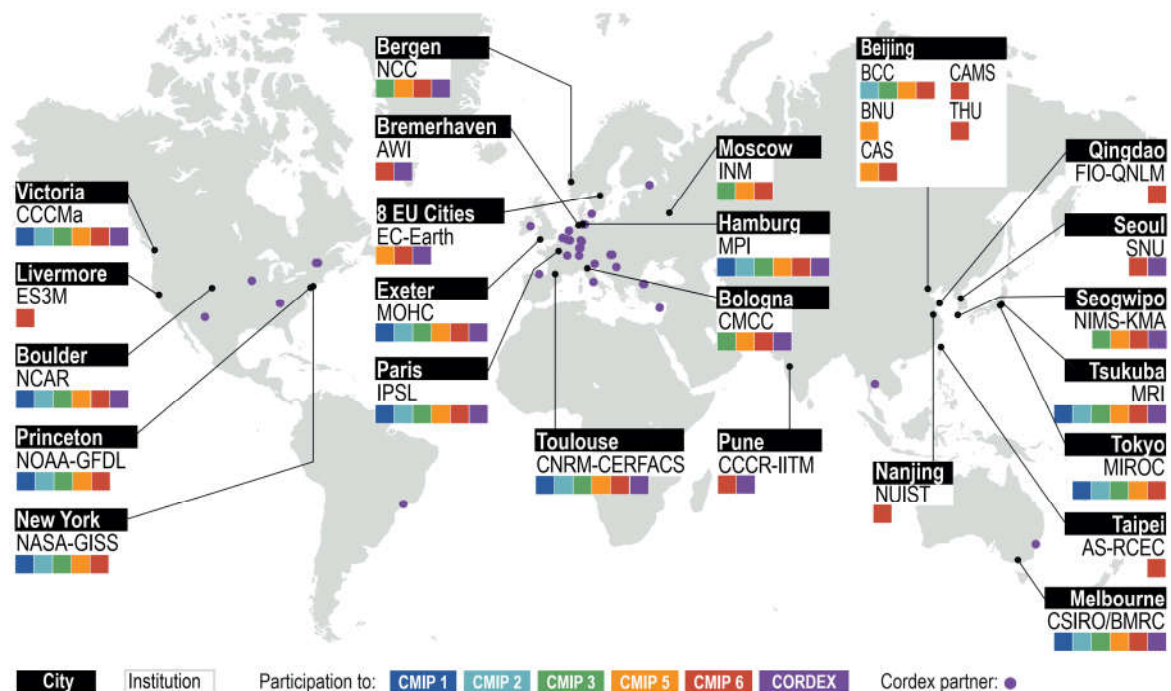
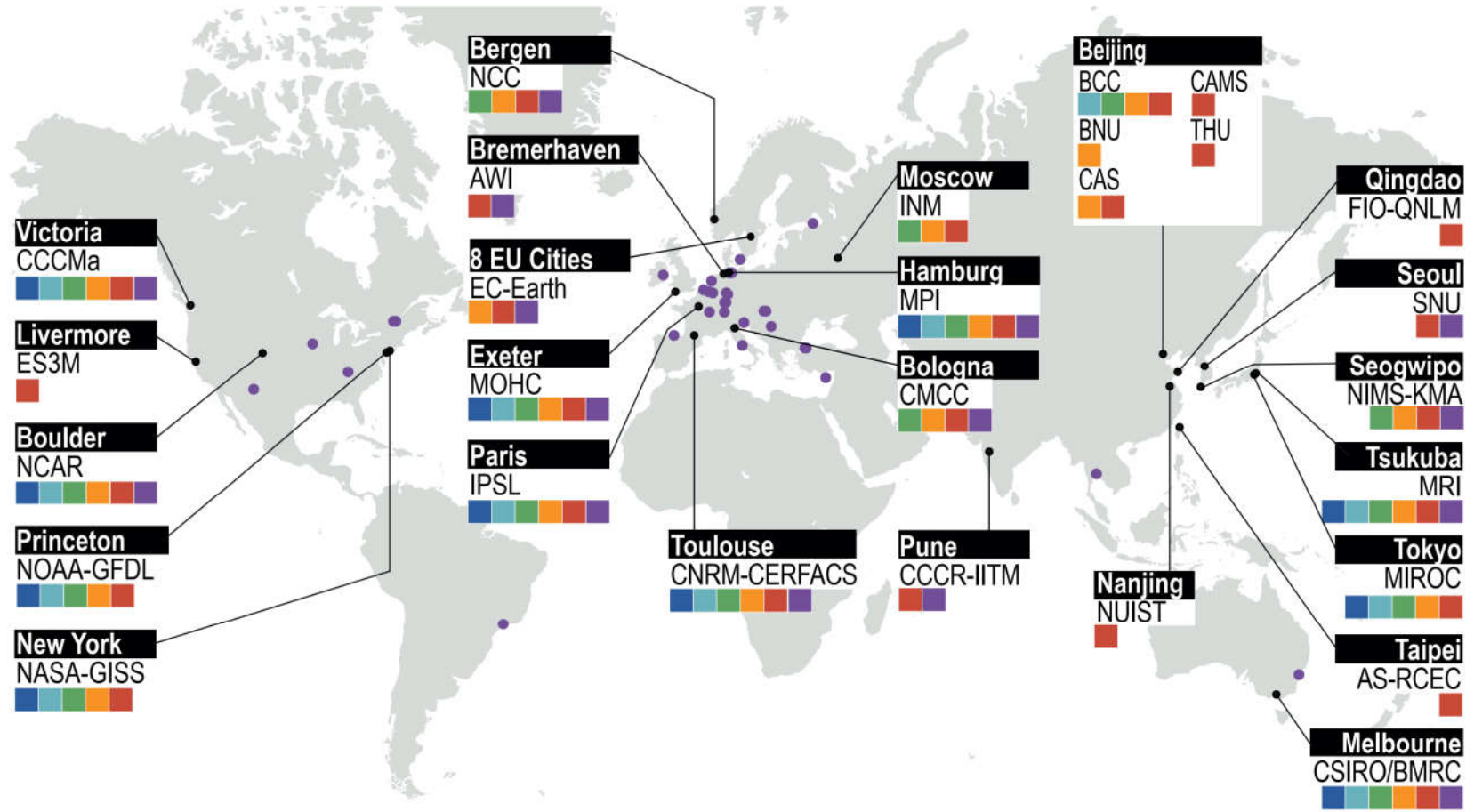


**Figure 1.20 | World map showing the increased diversity of modelling centres contributing to CMIP and CORDEX.** Climate models are often developed by international consortia. One such consortium, EC-Earth, is shown as an example under the label **8 EU Cities** (involving SMHI, Sweden; KNMI, The Netherlands; DMI, Denmark; AEMET, Spain; Met Éireann, Ireland; CNR-ISAC, Italy; Instituto de Meteorologia, Portugal; and FMI, Finland). There are too many such collaborations to display all of them on this map. More complete information about institutions contributing to CORDEX and CMIP6 is found in Annex II.



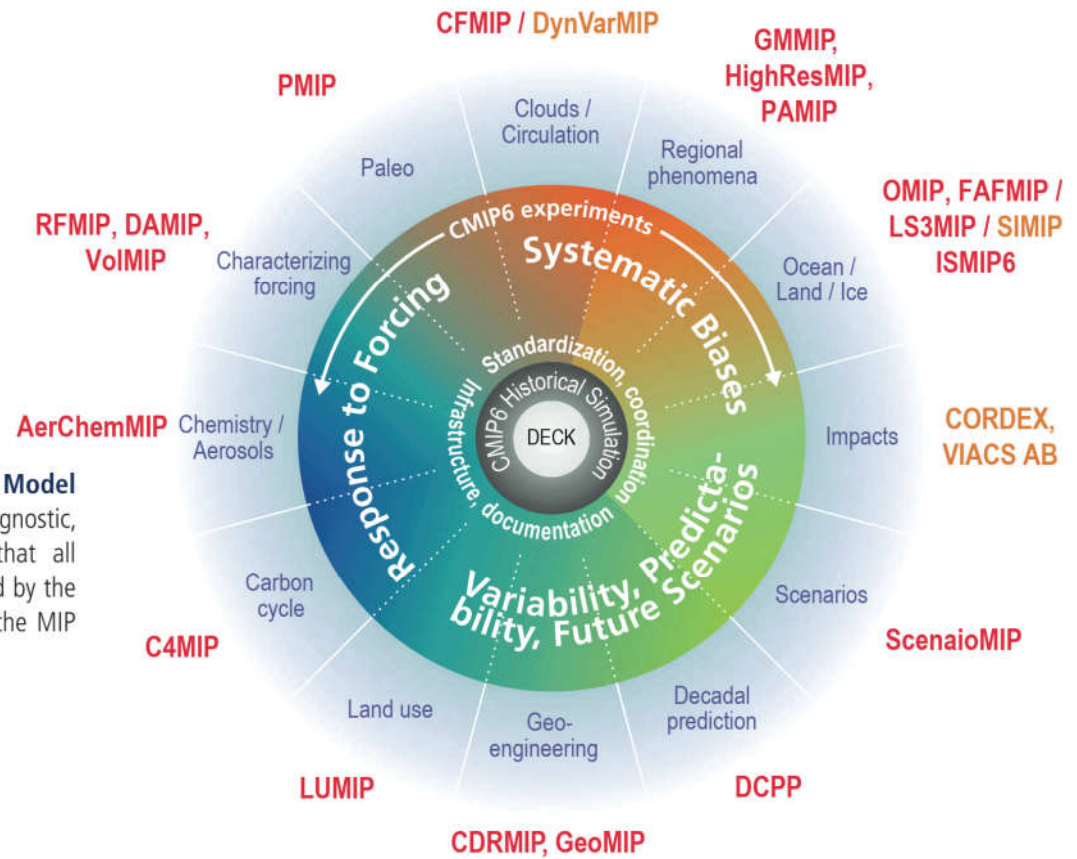
City Institution

Participation to: CMIP 1 CMIP 2 CMIP 3 CMIP 5 CMIP 6 CORDEX

Cordex partner: ●

# Structure of CMIP6, the 6th phase of the Coupled Model Intercomparison Project

**Figure 1.22 | Structure of CMIP6, the 6th phase of the Coupled Model Intercomparison Project.** The centre shows the common DECK (Diagnostic, Evaluation and Characterization of Klima) and historical experiments that all participating models must perform. The outer circles show the topics covered by the endorsed (red) and other MIPs (orange). See Table 1.3 for explanation of the MIP acronyms. Figure is adapted from Eyring et al. (2016).



# Resolution of the atmospheric and oceanic components of global climate models participating in CMIP5, CMIP6, and HighResMIP

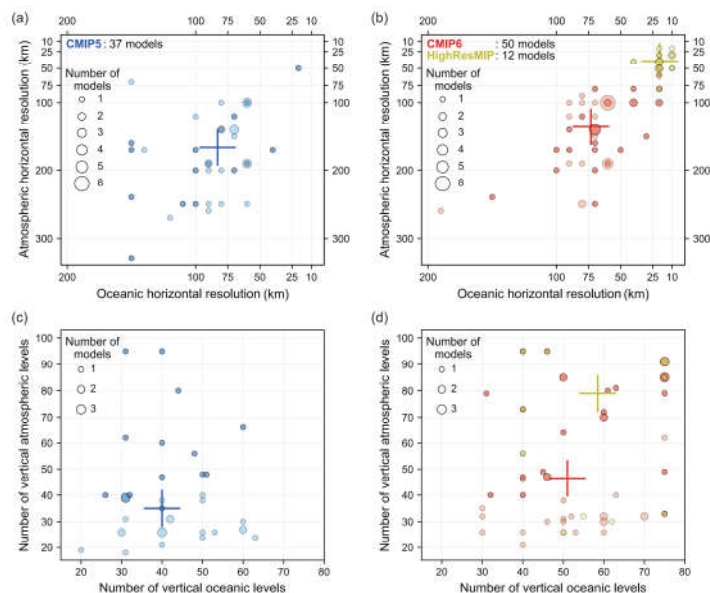


**Figure 1.19 | Resolution of the atmospheric and oceanic components of global climate models participating in CMIP5, CMIP6 and HighResMIP: (a, b) horizontal resolution (km), and (c, d) number of vertical levels.** Darker-colour circles indicate high-top models (in which the top of the atmosphere is above 50 km). The crosses are the median values. These models are documented in Annex II. Note that duplicated models in a modelling group are counted as one entry when their horizontal and vertical resolutions are the same. For HighResMIP, one atmosphere–ocean coupled model with the highest resolution from each modelling group is used. The horizontal resolution (rounded to 10 km) is the square root of the surface area of the Earth divided by the number of grid points, or the area of the ocean surface divided by the number of surface ocean grid points, for the atmosphere and ocean, respectively.

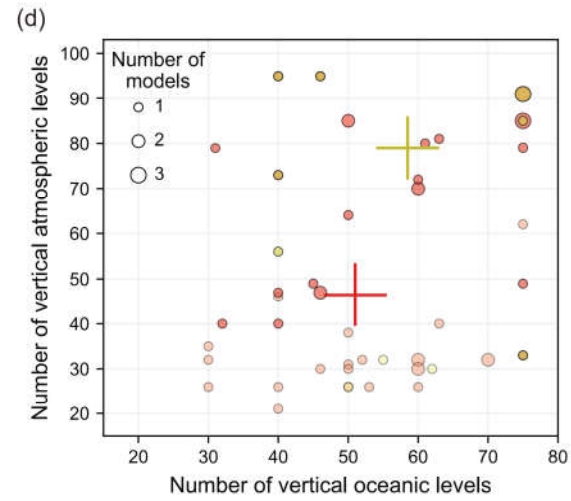
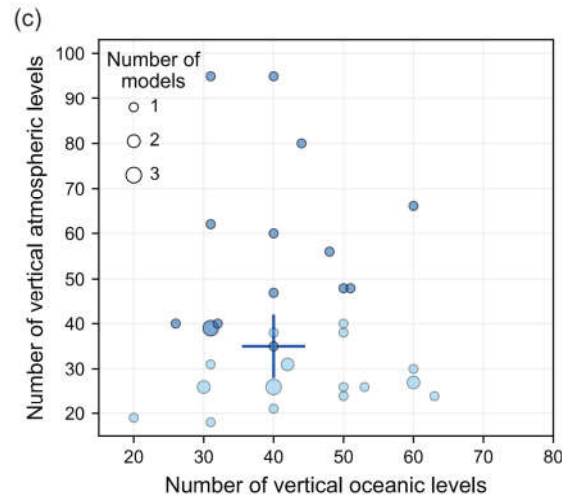
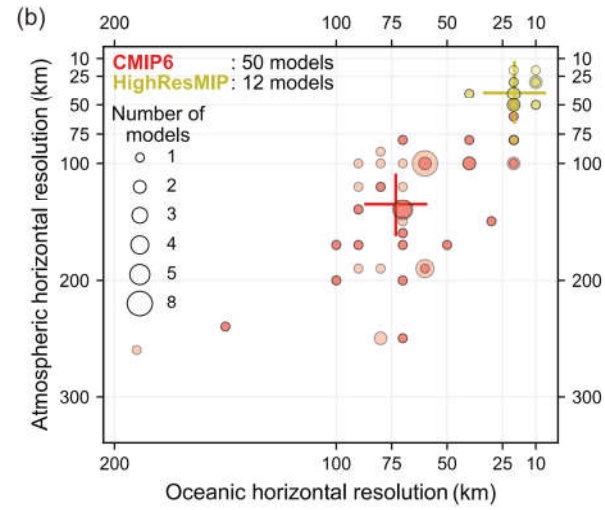
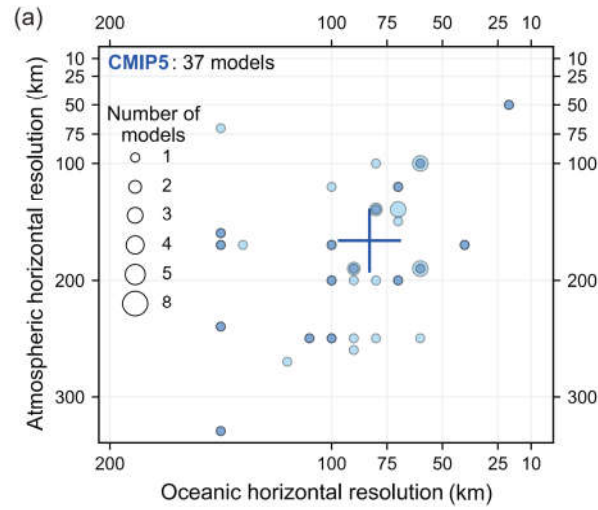


## Illustration of common types of model ensemble, simulating the time evolution of a quantity Q

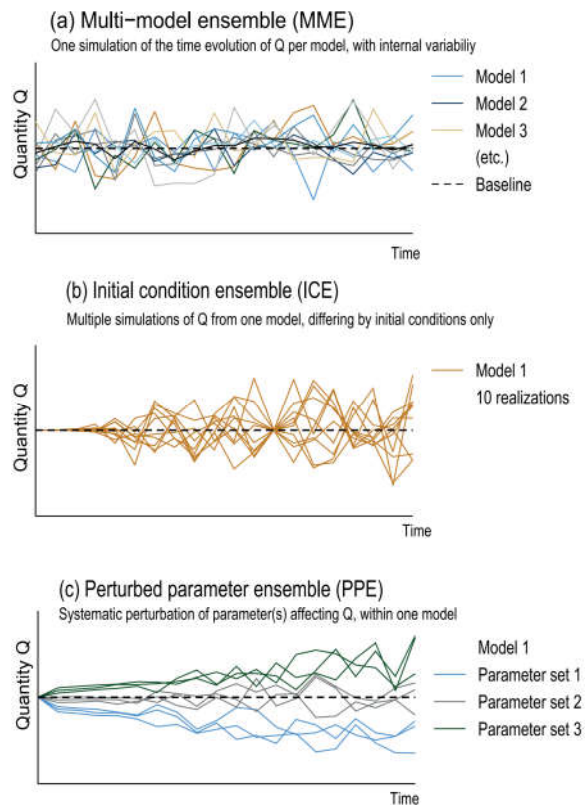


**Figure 1.21 | Illustration of common types of model ensemble, simulating the time evolution of a quantity Q (such as global mean surface temperature).** (a) Multi-model ensemble, where each model has its own realization of the processes affecting Q, and its own internal variability around the baseline value (dashed line). The multi-model mean (black) is commonly taken as the ensemble average. (b) Initial condition ensemble, where several realizations from a single model are compared. These differ only by minute ('micro') perturbations to the initial conditions of the simulation, such that over time, internal variability will progress differently in each ensemble member. (c) Perturbed physics ensemble, which also compares realizations from a single model, but where one or more internal parameters that may affect the simulations of Q are systematically changed to allow for a quantification of the impact of those quantities on the model results. Additionally, each parameter set may be taken as the starting point for an initial condition ensemble. In this figure, each set has three ensemble members.

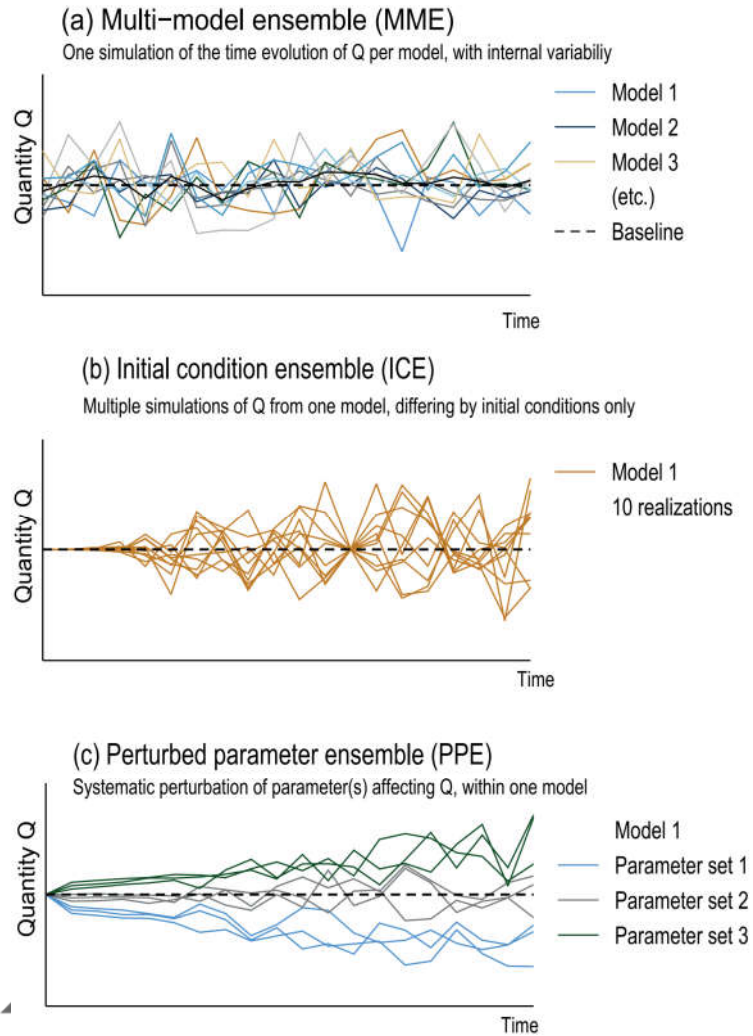


**Figure 1.21 | Illustration of common types of model ensemble, simulating the time evolution of a quantity Q (such as global mean surface temperature).**

**(a)** Multi-model ensemble, where each model has its own realization of the processes affecting Q, and its own internal variability around the baseline value (dashed line). The multi-model mean (black) is commonly taken as the ensemble average. **(b)** Initial condition ensemble, where several realizations from a single model are compared. These differ only by minute ('micro') perturbations to the initial conditions of the simulation, such that over time, internal variability will progress differently in each ensemble member. **(c)** Perturbed physics ensemble, which also compares realizations from a single model, but where one or more internal parameters that may affect the simulations of Q are systematically changed to allow for a quantification of the impact of those quantities on the model results. Additionally, each parameter set may be taken as the starting point for an initial condition ensemble. In this figure, each set has three ensemble members.



## Statements in the Executive Summary

### Data, Tools and Methods Used across the WGI Report (5)

**Assessments of future climate change are integrated within and across the three IPCC Working Groups through the use of three core components: scenarios, global warming levels, and the relationship between cumulative carbon emissions and global warming.** Scenarios have a long history in the IPCC as a method for systematically examining possible futures. A new set of scenarios, derived from the Shared Socio-economic Pathways (SSPs), is used to synthesize knowledge across the physical sciences, impact, and adaptation and mitigation research. The core set of SSP scenarios used in the WGI report, SSP1-1.9, SSP1-2.6, SSP2-4.5, SSP3-7.0 and SSP5-8.5, cover a broad range of emission pathways, including new low-emissions pathways. The feasibility or likelihood of individual scenarios is not part of this assessment, which focuses on the climate response to possible, prescribed emission futures. Levels of global surface temperature change (global warming levels), which are closely related to a range of hazards and regional climate impacts, also serve as reference points within and across IPCC Working Groups. Cumulative carbon emissions, which have a nearly linear relationship to increases in global surface temperature, are also used. {1.6.1-1.6.4, Cross-Chapter Box 1.5, Cross-Chapter Box 11.1}

*IPCC 2021, Chap. 1*





# A simplified illustration of the scenario generation process

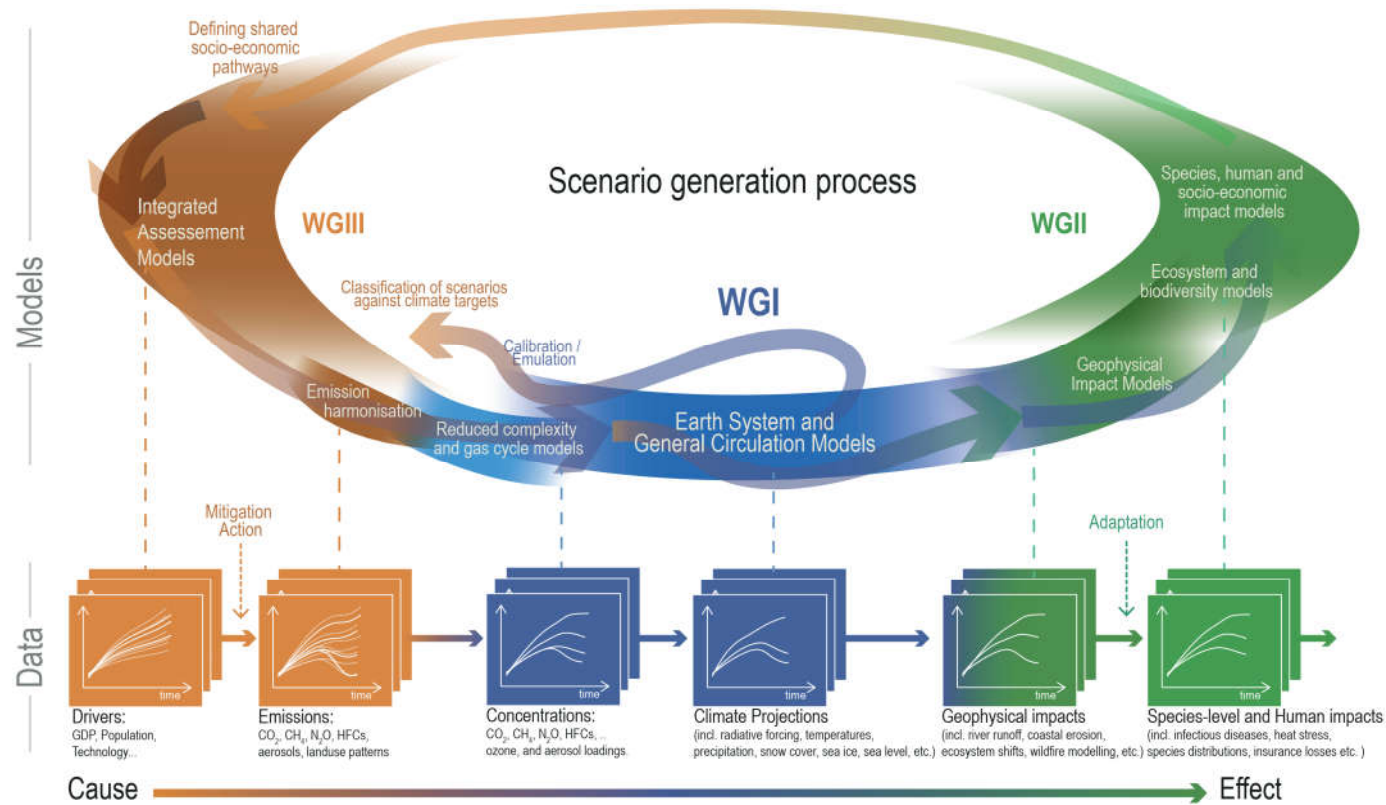
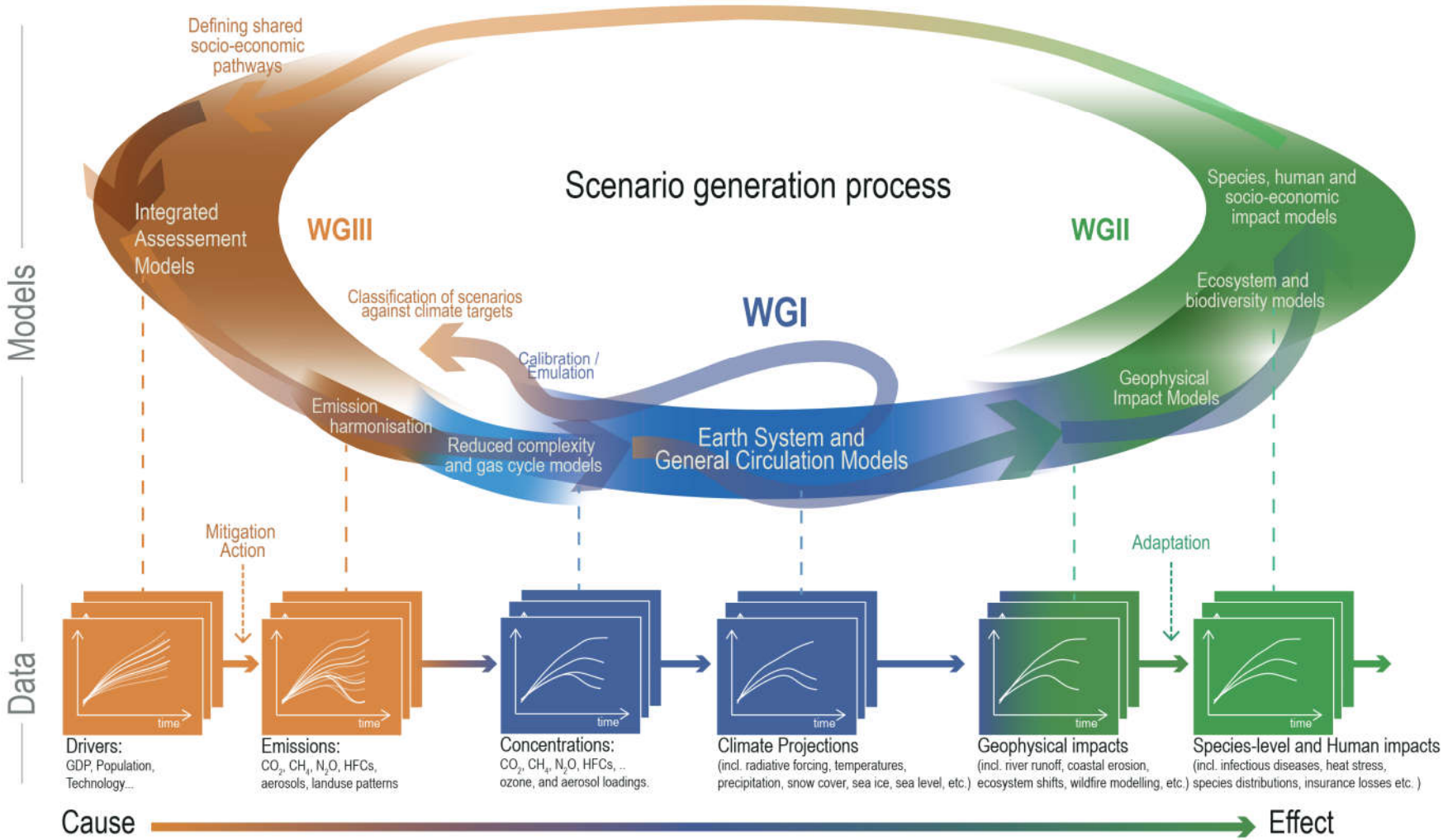
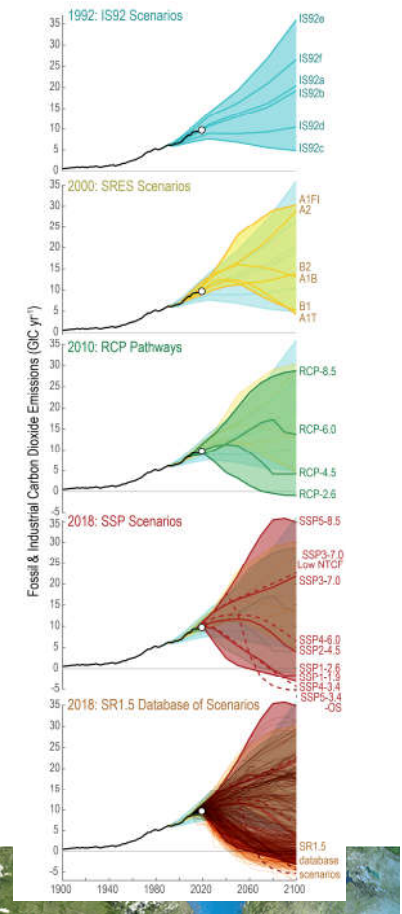


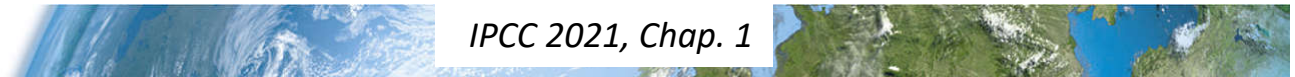
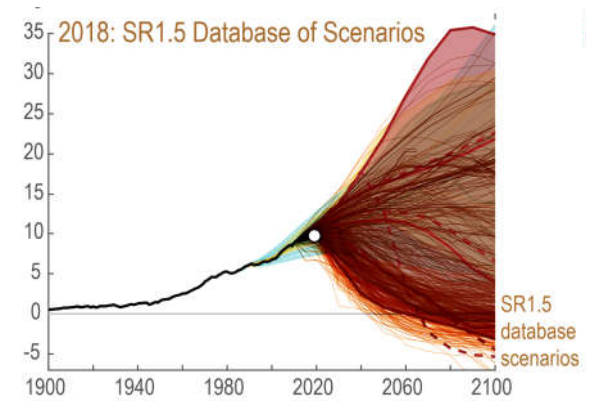
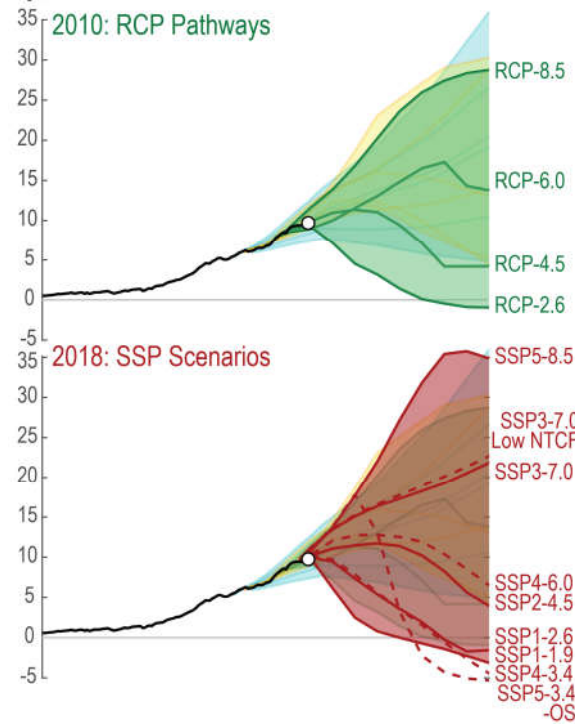
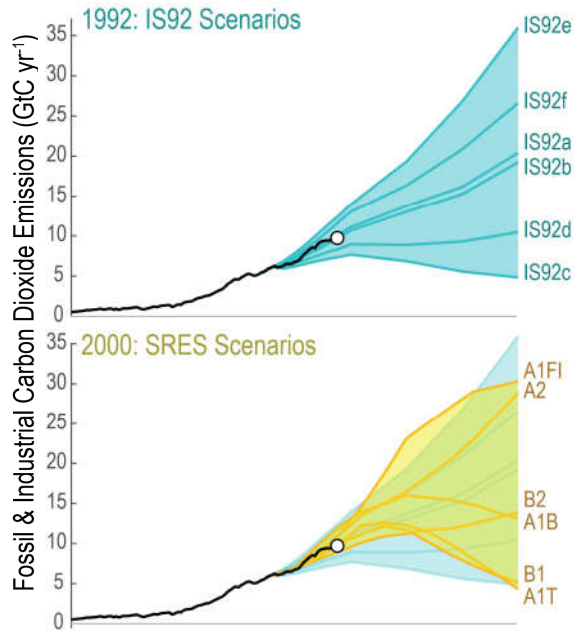
Figure 1.27 | A simplified illustration of the scenario generation process, involving the scientific communities represented in the three IPCC Working Groups. The circular set of arrows at the top indicates the main set of models and workflows used in the scenario generation process, with the lower level indicating the datasets.



# Comparison of the range of fossil and industrial CO<sub>2</sub> emissions from scenarios used in previous assessments up to AR6.

**Figure 1.28 | Comparison of the range of fossil fuel and industrial CO<sub>2</sub> emissions from scenarios used in previous assessments up to AR6.** Previous assessments are the IS92 scenarios from 1992 (**top**), the Special Report on Emissions Scenarios (SRES) scenarios from the year 2000 (**second panel**), the Representative Concentration Pathway (RCP) scenarios designed around 2010 (**third panel**) and the Shared Socio-economic Pathways (SSP) scenarios (**fourth panel**). In addition, historical emissions are shown (black line; Figure 5.5); a more complete set of scenarios is assessed in SR1.5 (**bottom**); (Huppmann et al., 2018). Further details on data sources and processing are available in the chapter data table (Table 1.SM.1).





# The Dimensions of Integration across Chapters and Working Groups in the IPCC AR6 assessment

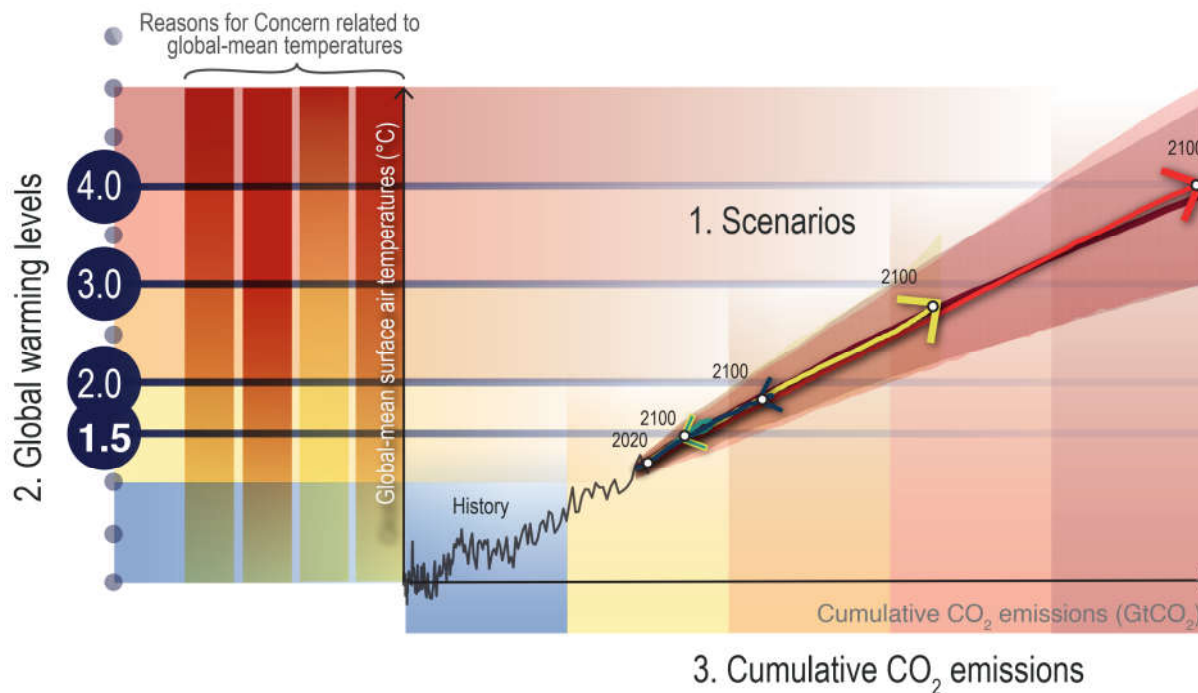
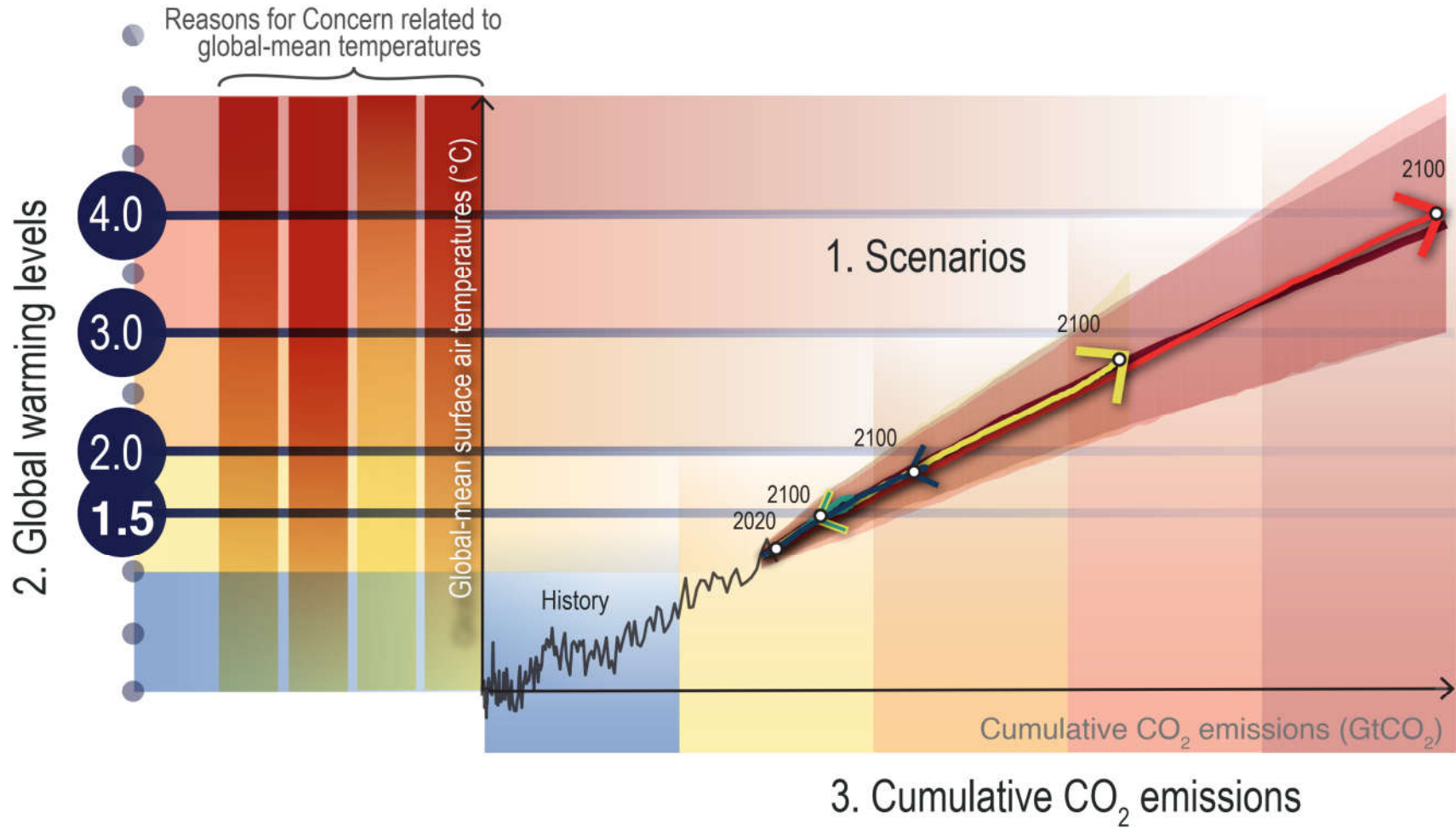
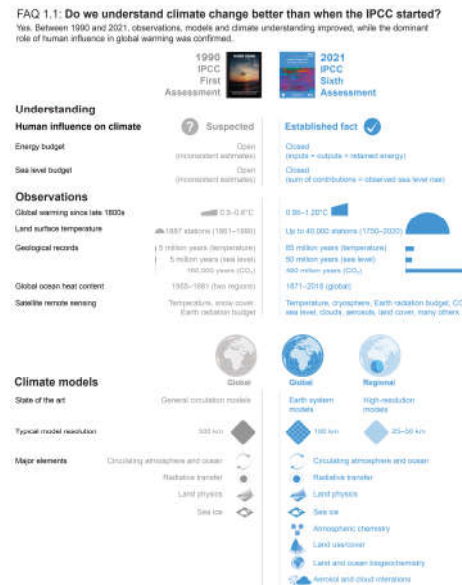


**Figure 1.24 | The dimensions of integration across chapters and Working Groups in the IPCC AR6 Assessment.** This Report adopts three explicit dimensions of integration to integrate knowledge across chapters and Working Groups. The first dimension is scenarios; the second dimension is global mean warming levels relative to pre-industrial levels; and the third dimension is cumulative CO<sub>2</sub> emissions. For the scenarios, illustrative 2100 end-points are also indicated (white circles). Further details on data sources and processing are available in the chapter data table (Table 1.SM.1).



# Sample elements of climate understanding, observations and models as assessed in the IPCC First Assessment Report (1990) and Sixth Assessment Report (2021)



**FAQ 1.1, Figure 1 | Sample elements of climate understanding, observations and models as assessed in the IPCC First Assessment Report (1990) and Sixth Assessment Report (2021).** Many other advances since 1990, such as key aspects of theoretical understanding, geological records and attribution of change to human influence, are not included in this figure because they are not readily represented in this simple format. Fuller explanations of the history of climate knowledge are available in the introductory chapters of the IPCC Fourth and Sixth assessment reports.



## FAQ 1.1: Do we understand climate change better than when the IPCC started?

Yes. Between 1990 and 2021, observations, models and climate understanding improved, while the dominant role of human influence in global warming was confirmed.



### Understanding

#### Human influence on climate

Energy budget

**? Suspected**

Open  
(inconsistent estimates)

**Established fact** ✓

Closed  
(inputs = outputs + retained energy)

Sea level budget

Open  
(inconsistent estimates)

Closed  
(sum of contributions = observed sea level rise)

### Observations

Global warming since late 1800s

0.3–0.6°C

0.95–1.20°C

Land surface temperature

1887 stations (1861–1990)

Up to 40,000 stations (1750–2020)

Geological records

5 million years (temperature)  
5 million years (sea level)  
160,000 years (CO<sub>2</sub>)

65 million years (temperature)  
50 million years (sea level)  
450 million years (CO<sub>2</sub>)

Global ocean heat content

1955–1981 (two regions)

1871–2018 (global)

Satellite remote sensing

Temperature, snow cover,  
Earth radiation budget

Temperature, cryosphere, Earth radiation budget, CO<sub>2</sub>,  
sea level, clouds, aerosols, land cover, many others







## Climate models

State of the art



General circulation models

Typical model resolution

500 km



Major elements

Circulating atmosphere and ocean



Radiative transfer



Land physics



Sea ice



Global

Earth system models



100 km



Regional

High-resolution models



25–50 km



Circulating atmosphere and ocean



Radiative transfer



Land physics



Sea ice



Atmospheric chemistry



Land use/cover



Land and ocean biogeochemistry



Aerosol and cloud interactions



## Chapter 2: Changing state of the climate system

Nächste Vorlesung am 9. November 2021



Knowledge for Tomorrow